Clinical Science (2022) **136** 657–673
https://doi.org/10.1042/CS20220043

PORTLAND PRESS

Research Article

ANGPTL1 attenuates cancer migration, invasion, and stemness through regulating FOXO3a-mediated SOX2 expression in colorectal cancer

Ting-Yu Chang[1], Kuo-Cheng Lan[2], Chen-Yuan Chiu[3], Meei-Ling Sheu[4,5] and Shing-Hwa Liu[1,6,7]

[1]Graduate Institute of Toxicology, College of Medicine, National Taiwan University, Taipei, Taiwan; [2]Department of Emergency Medicine, Tri-Service General Hospital, National Defense Medical Center, Taipei, Taiwan; [3]Center of Consultation, Center for Drug Evaluation, Taipei, Taiwan; [4]Institute of Biomedical Sciences, National Chung Hsing University, Taichung, Taiwan; [5]Department of Medical Research, Taichung Veterans General Hospital, Taichung, Taiwan; [6]Department of Medical Research, China Medical University Hospital, China Medical University, Taichung, Taiwan; [7]Department of Pediatrics, College of Medicine, National Taiwan University & Hospital, Taipei, Taiwan

Correspondence: Meei-Ling Sheu (mlsheu@nchu.edu.tw) or Shing-Hwa Liu (shinghwaliu@ntu.edu.tw)

Angiopoietin-like protein 1 (ANGPTL1) is a member of the ANGPTL family that suppresses angiogenesis, cancer invasion, metastasis, and cancer progression. ANGPTL1 is down-regulated in various cancers including colorectal cancer (CRC); however, the effects and mechanisms of ANGPTL1 on liver metastasis and cancer stemness in CRC are poorly understood. In the present study, we identified that ANGPTL1 was down-regulated in CRC and inversely correlated with metastasis and poor clinical outcomes in CRC patients form the ONCOMINE database and Human Tissue Microarray staining. ANGPTL1 significantly suppressed the migration/invasion abilities, the expression of cancer stem cell (CSC) markers, and sphere formation by enhancing FOXO3a expression, which contributed to the reduction of stem cell transcription factor SOX2 expression in CRC cells. Consistently, overexpression of ANGPTL1 reduced liver metastasis, tumor growth, and tumorigenicity in tumor-bearing mice. ANGPTL1 expression was negatively correlated with CSC markers expression and poor clinical outcomes in CRC patients. Taken together, these findings demonstrate that the molecular mechanisms of ANGPTL1 in colorectal cancer stem cell progression may provide a novel therapeutic strategy for CRC.

Introduction

Colorectal cancer (CRC) is a major diagnosed cancer and the third leading cause of death and disease from cancer worldwide [1]. Approximately 50% of patients with CRC developed distant metastases, and the 5-year survival rates were low in those patients [1]. Both recurrence and metastasis are two important prognosis factors for survival of colon cancer. Therefore, it is vital and urgent to investigate the genes and detailed molecular mechanisms involved in CRC tumor metastasis, which may provide novel diagnostic biomarkers for CRC. Increasing evidences have implicated that cancer stem cells (CSCs) participate in tumor initiation, metastasis, drug resistance, and tumor recurrence [2–5]. CSCs exhibit as small subpopulations of tumor cells resides in niches, which is a part of the tumor microenvironment and supports cancer cell dissemination [6]. Recent studies have reported that some cancer cells, including CRC, acquire the features of CSCs through the epithelial–mesenchymal transition (EMT), which facilitate the invasion potential of colon cancer cells into the basement membrane and the lymph and blood vascular systems [7,8]. Due to the plasticity and capacity of CSCs, it is essential for developing the therapeutic strategies to eliminate CSCs for CRC therapy.

Angiopoietin-like protein 1 (ANGPTL1) is a member of ANGPTLs family and known as an anti-angiogenic factor as well as a tumor suppressor. Indeed, ANGPTL1 is down-regulated in several cancers, including lung [9], thyroid [10], hepatocellular carcinoma [11] and colorectal cancer [12]. ANGPTL1

Received: 18 January 2022
Revised: 26 April 2022
Accepted: 26 April 2022

Accepted Manuscript online: 27 April 2022
Version of Record published: 06 May 2022

Clinical Science (2022) **136** 657–673
https://doi.org/10.1042/CS20220043

is implicated in the angiogenesis [11], metastasis [13], inflammation [14], hematopoietic stem cell behavior [15], lipid metabolism [16], drug resistance [17] and cancer progression [18]. Previous studies showed that ANGPTL1 repressed EMT by inhibiting Slug expression of CRC [9], and proved that ANGPTL1 suppressed liver metastasis and prolonged overall survival *in vivo* of CRC [12]. In hepatocellular carcinoma (HCC), ANGPTL1 attenuates cancer stem cell properties and sorafenib resistance by reduction of Slug [17]. Nevertheless, the functions and detailed mechanisms of ANGPTL1 in CSC properties of CRC are yet not fully developed.

In the present study, we investigated the effects and mechanisms of ANGPTL1 on liver metastasis and cancer stemness in CRC. We demonstrate a novel mechanism in which ANGPTL1 inhibits SRY-related HMG-box (SOX)-2 (SOX2) expression by enhancing forkhead box O (FOXO)-3a (FOXO3a) expression, thereby reduces migration, invasion, liver metastasis, and cancer stemness of CRC. Furthermore, the tumorigenicity was eliminated in ANGPTL1-overexpressed tumors *in vivo* and ANGPTL1 expression was inversely correlated with the expression of cancer stem cell markers, and conferred better clinical outcomes in patients with CRC. These findings not only illustrate how ANGPTL1 reduces CRC metastasis and cancer stemness but provides a rationale for developing the potential therapeutic strategy of ANGPTL1 for CRC patients.

Materials and methods

Immunohistochemistry (IHC) staining

CRC human tissue microarrays (TMA) were purchased form SuperBioChips (Seoul, Korea), including 59 paired normal colon and rectum tissues (CDN4) and tumor tissues (CD4), and human CRC metastasis-normal tissues (CDA3). IHC staining was performed by an IHC kit (cat. no. ab64264, Abcam, Cambridge, U.K.) with the manufacturer's instructions. Briefly, TMA sections were deparaffinized and rehydrated in gradient ethanol solutions. For antigen retrieval, slides were incubated with protease and blocked with protein block reagent for 10 min, and then incubated with ANGPTL1 antibody (1:100; cat. no. sc-271841, Santa Cruz Biotechnology, Dallas, TX, U.S.A.) overnight at 4 °C. Slides were applied for HRP-conjugated secondary antibody, incubated with DAB substrate, counterstained with hematoxylin, and mounted with mounting medium. Finally, slides were measured by ImageJ software with the IHC profiler plugin [19]. Two groups were analyzed: lower expression (score 0 and 1) and higher expression (score 2 and 3). The negative staining is score 0; the positive staining in $\leq$ 20% is score 1; the positive staining in 20%∼50% is score 2; strong staining in >50% is score 3.

Cell lines

Both SW480 and SW620 cells were grown in DMEM/F12 medium. HT-29 cells were grown in DMEM medium. American Type Culture Collection (ATCC; Manassas, VA, U.S.A.) provided these cell lines. HCT116 cell were grown in McCoy's 5A medium and purchased from the Bioresource Collection and Research Center (BCRC, Hsinchu, Taiwan). Media were supplemented with 1% penicillin-streptomycin-Amphotericin B and 10% fetal bovine serum (FBS), incubated at 37°C with 5% CO_2. These cells have been checked for free of mycoplasma contamination.

Immunoblotting and antibodies

Cells were lysed in RIPA lysis buffer supplemented with protease inhibitor cocktail (cat. no. 78430, Thermo Fisher Scientific, Waltham, MA, U.S.A.). It was then centrifuged at 13,000 rpm for 30 min. Protein samples were mixed with gel sample buffer, separated by SDS–polyacrylamide gel electrophoresis, transferred to a PVDF membrane (Merck Millipore, Billerica, MA, U.S.A.), blocked, incubated with primary antibodies, and secondary antibodies. The immunoreactive proteins were identified by reaction with enhanced ECL system (Bio-Rad, Hercules, CA, U.S.A.). The primary antibodies were used for ANGPTL1 (cat. no. sc-271841, Santa Cruz Biotechnology), SOX2 (cat. no. #3579, Cell Signaling Technology, Danvers, MA, U.S.A.), Oct4 (cat. no. #2750, Cell Signaling Technology), Nanog (cat. no. ab80892, Abcam), LGR5 (cat. no. ab273092, Abcam), CD133 (cat. no. #64326, Cell Signaling Technology), FOXO1 (cat. no. sc-11350, Santa Cruz Biotechnology), FOXO3a (cat. no. ab53287, Abcam), FOXO4 (cat. no. #9472, Cell Signaling Technology), and α-Tubulin (cat. no. T-5168; Sigma-Aldrich). The secondary antibodies for immunoblotting were obtained from Cell Signaling Technology.

Transwell migration and invasion assay

Migration and invasion abilities were assessed as previously described [20]. Briefly, cells were plated inside the upper chamber in medium without serum, and the lower chamber contained medium with 10% FBS as a chemoattractant at a 24-well plate. The 8×10^4 cells were seeded in the upper chamber and incubated for 24 h for migration assay. For invasion assay, the transwell chamber coated with Matrigel matrix (Corning Costar, Lowell, MA, U.S.A.) was used.

The 1×10^5 cells were seeded in the upper chamber and incubated for 24 h. Cells were removed by cotton swabs in the upper chamber, and cells on the membrane surface of the lower chamber were fixed and stained by Crystal Violet (0.05%). The ImageJ software was used for quantification.

Sphere formation assay

Sphere formation was determined as previously described [20]. Cells were seeded on the ultra–low attachment 24-well plates (Corning Costar) with sphere formation medium, which was contained serum free culture medium, B27 supplement, recombinant human EGF (20 ng/ml), and basic FGF (10 ng/ml) for 14 days. The diameters of spheres reached 50 μm were counted.

Plasmid constructs, RNA interference, cell transfection, and virus infection assay

Full-length human ANGPTL1 was cloned into the pcDNA3.1/V5-His Topo vector (Thermo Fisher Scientific). The SOX2 small interfering RNA (siRNA) in a TriFECTa RNAi Kit was obtained from Integrated DNA Technologies (Coralville, IA, U.S.A.). Cell transfection was performed with PrueFection reagent (System Biosciences, Palo Alto, CA, U.S.A.). Experiments were conducted following the manufacturer's instruction. The lentivirus ANGPTL1 short hairpin RNA (shRNA) clones (TRCN0000426666 and TRCN0000434824), FOXO3 shRNA clones (TRCN0000235488 and TRCN0000235490), pLKO.1-emptyT control clone (TRCN0000208001), and plasmids for pMD2.G and pCMV-deltaR8.91 were obtained from the National RNAi Core Facility at Academia Sinica (Taipei, Taiwan). For lentivirus preparation, HEK-293T cells were transfected with 3.5 μg plasmid DNA, 0.35 μg of envelop plasmid (pMD2.G) and 3.15 μg of package plasmid (pCMV-deltaR8.91) using PureFection reagent. The medium contained lentivirus was collected after 48 h, centrifuged at 1250 rpm for 5 min, and then the supernatant was collected. Cells were infected with medium containing lentivirus and supplemented with 8 μg/ml polybrene (cat. no. H9268, Sigma-Aldrich) for 48 h.

Animals

Male nude mice (5 weeks old) were purchased from BioLASCO (Taipei, Taiwan) and maintained in accordance with the Guide of Association for Assessment and Accreditation of Laboratory Animal Care International. All animal experiments were approved by the Institutional Animal Care and Use Committee at the National Taiwan University College of Medicine (Taipei, Taiwan) (IACUC No. 20200023). Animals were acclimatized and housed under pathogen-free conditions for one week before the experiments. All surgeries were carried out in an operating room at the Laboratory Animal Center of the National Taiwan University College of Medicine.

Intrasplenic injection model

The liver metastasis of CRC was evaluated by an intrasplenic injection model. The 1×10^5 cells were suspended in 50 μl PBS and gently injected into the exposed spleens of mice with a 31G needle ($n = 7$/ group) under anesthesia (Zoletil 50 mg/kg/Xylazine 2 mg/kg mixture, i.p.), then the peritoneum was closed with stitch. Four weeks later, the mice were killed and the liver were excised to examine and quantify the amount of liver metastasis.

Tumor xenograft animal model

For tumor growth assay, 5×10^6 tumor cells were suspended in PBS contained equal volume of Matrigel (BD Biosciences, San Jose, CA, U.S.A.) on ice and subcutaneously inoculated into the dorsal flanks of mice ($n = 8$/group). For tumorigenesis assay, the indicated number of cells were subcutaneously injected into mice ($n = 8$/group). Tumor volumes were detected twice a week using a caliper and calculated following the formula [(length × width × width) /2].

Statistical analysis

All data are presented as the mean ± S.D. from at least 3 independent experiments using a Prism 6 software (GraphPad, San Diego, CA, U.S.A.). The significant difference among multi-groups was analyzed by a one-way ANOVA with Tukey's post-hoc test. $P<0.05$ were statistically significant.

Clinical Science (2022) **136** 657–673
https://doi.org/10.1042/CS20220043

Table 1 Clinic pathological features, clinical outcomes and their association with *ANGPTL1* expression in colorectal cancer datasets

Clinic pathological features	Datasets	Mean *ANGPTL1* expression (normal tissues)	Mean *ANGPTL1* expression (tumor tissues)	Fold change*	*P*-value†
Rectal adenocarcinoma	Gaedcke (*n*=65)	1.89	−0.77	−6.321	1.44×10^{-48}
	Kaiser (*n*=8)	−0.34	−0.68	−1.697	0.002
	TCGA (*n*=60)	4.67	−0.30	−21.740	2.42×10^{-21}
Colon adenocarcinoma	Kaiser (*n*=41)	−0.34	−0.92	−2.306	8.84×10^{-7}
	TCGA (*n*=102)	4.67	−0.23	−19.706	4.00×10^{-19}
Colorectal adenocarcinoma	Skrzypczak (*n*=45)	0.50	−0.88	−2.945	1.48×10^{-7}
	Hong (*n*=70)	−1.28	−3.22	−8.882	1.93×10^{-6}
Recurrence at 5 years	Jorissen (*n*=56)	−1.1	−1.9	−1.630	0.024

*Fold change (Log2 median-centered intensity).
†*P*-value of individual dataset were obtained from the ONCOMINE database.

Results

ANGPTL1 expression was down-regulated in CRC and associated with better prognosis

To determine the clinical significance of ANGPTL1 in CRC, we queried the ONCOMINE database to define *ANGPTL1* gene expression in CRC patients (1.5-fold change, P-value < 0.05 as the threshold) and observed that *ANGPTL1* was highly expressed in normal tissues, non-metastatic tissue, and associated with low recurrence in patients (Figure 1A). We also analyzed other datasets of CRC patients and found that *ANGPTL1* expression was down-regulated in CRC patients and inversely correlated with poor outcomes (Table 1). Moreover, we detected ANGPTL1 expression of normal colon and CRC tissues using CRC tissue microarrays (TMAs), which contained 59 paired normal and tumor tissues, and 10 CRC tissues with or without metastasis. The different scores of ANGPTL1 were represented in Figure 1B based on IHC staining analysis. The results showed that ANGPTL1 expression levels were higher in normal colon tissues than paired CRC tissues (Figure 1C), and elevated ANGPTL1 expression had longer survival outcomes in CRC patients by Kaplan–Meier survival analysis (Figure 1D). Compared with metastatic CRC tissues, the scores of ANGPTL1 staining were higher in paired non-metastatic CRC tissues (Figure 1E). These results suggest that ANGPTL1 inversely correlates with worse prognosis in CRC patients.

ANGPTL1 suppresses CRC cell malignant mobility and metastasis

To validate the metastatic capacity of ANGPTL1 in CRC cells, we examined the expression of ANGPTL1 in both SW480 and SW620 cells. SW620 cells were derived from a lymph node metastasis of SW480 cells at the same patient [21]. Interestingly, the basal expression level of ANGPTL1 was lower in SW620 cells than SW480 cells (Figure 2A). To further determine the role of ANGPTL1 on cell mobility *in vitro*, we performed transwell migration and invasion assays. We knocked down ANGPTL1 in SW480 and HT-29 cells using shRNA lentivirus infection (Figure 2B), the migration and invasion abilities were significantly enhanced (Figure 2C–E). In contrast, overexpression of ANGPTL1 in highly metastatic SW620 and HCT116 cells dramatically inhibited the migration and invasion abilities in both SW620 and HCT116 cells (Figure 2F–I), implying that ANGPTL1 may suppress CRC cell mobility.

The intrasplenic injection model has been suggested to be a reliable *in vivo* experimental metastasis assay for testing the cancer stem cell seeding capacity or metastatic stem cell property [22]. To evaluate the potential of ANGPTL1 on metastasis of CRC *in vivo*, we constructed an intrasplenic injection model using injection with HCT116/Vector or HCT116/ANGPTL1 cells into the spleens of nude mice. After four weeks, the liver metastatic nodules were significantly lower in ANGPTL1-transfected mice compared with the vector control mice (Figure 3A,B). The relative liver weight (normalized with body weight) was also lower (Figure 3C), and the body weight before euthanasia was higher in ANGPTL1-transfected mice (Figure 3D). In addition, a subcutaneous xenograft model was also performed with implanting the same groups into the dorsal flanks and measured the tumor volume and weight of the resulting primary tumors. Overexpression of ANGPTL1 markedly decelerated the tumor volume and weight compared with the control groups (Figure 3E,F). Taken together, these results indicate that ANGPTL1 impedes CRC metastasis *in vitro* and *in vivo*.

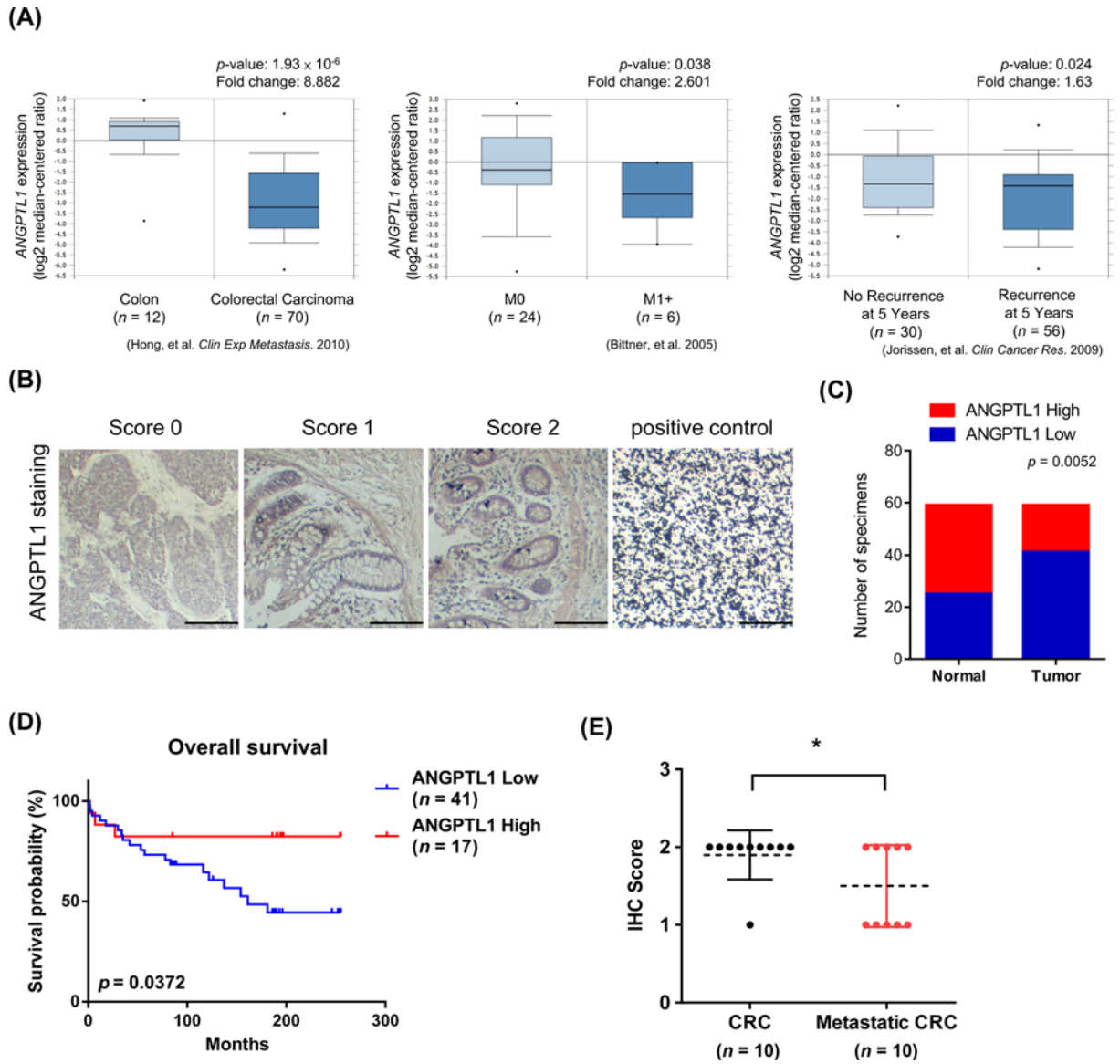

Figure 1. The clinical significance of ANGPTL1 expression in colorectal cancer (CRC)

(**A**) The expression of *ANGPTL1* negatively correlates with CRC, metastatic stage, and recurrence. ONCOMINE datasets: Hong_Colon, Bitner_Colon, and Jorissen_Colon. (**B**) IHC staining of ANGPTL1 in colon and CRC TMA tissues with scores of 0–3 was represented. Positive control: Carbon; scale bar: 100 μm. (**C**) The box plot representation of scores based on IHC staining of ANGPTL1 in 59 paired specimens of CRC and adjacent normal colon tissues. *P*-value was analyzed by Chi-square analysis followed by Fisher's exact test. (**D**) The overall survival of 58 patients in TMA with low and high ANGPTL1 expression was analyzed by Kaplan–Meier analysis ($P=0.0372$). ANGPTL1 expression was grouped based on the median of the IHC score of specimens. (**E**) ANGPTL1 expression inversely associated with metastatic tissues compared with paired specimens of CRC tissues in TMA ($n=10$). $^{*}P<0.05$ was obtained by paired two-tailed Student's *t*-tests.

ANGPTL1 diminishes the cancer stem cell (CSC) properties

CSCs are demonstrated that can be responsible for tumor progression, drug resistance, and metastasis due to their capacity, such as self-renewing and tumorigenicity [8]. Therefore, we verified the expression of CSC markers, including SOX2, Oct4, Nanog, LGR5, and CD133. All these markers were down-regulated in ANGPTL1-overexpressed cells, but dramatically induced in ANGPTL1-silenced cells (Figure 4A). Consistently, overexpression of ANGPTL1 significantly inhibited the sphere formation (Figure 4B). Of note, we further detected the expression of CSC markers of sphere cells and found that the CSC-related markers levels were decreased in ANGPTL1-overexpressed sphere cells

Clinical Science (2022) **136** 657–673
https://doi.org/10.1042/CS20220043

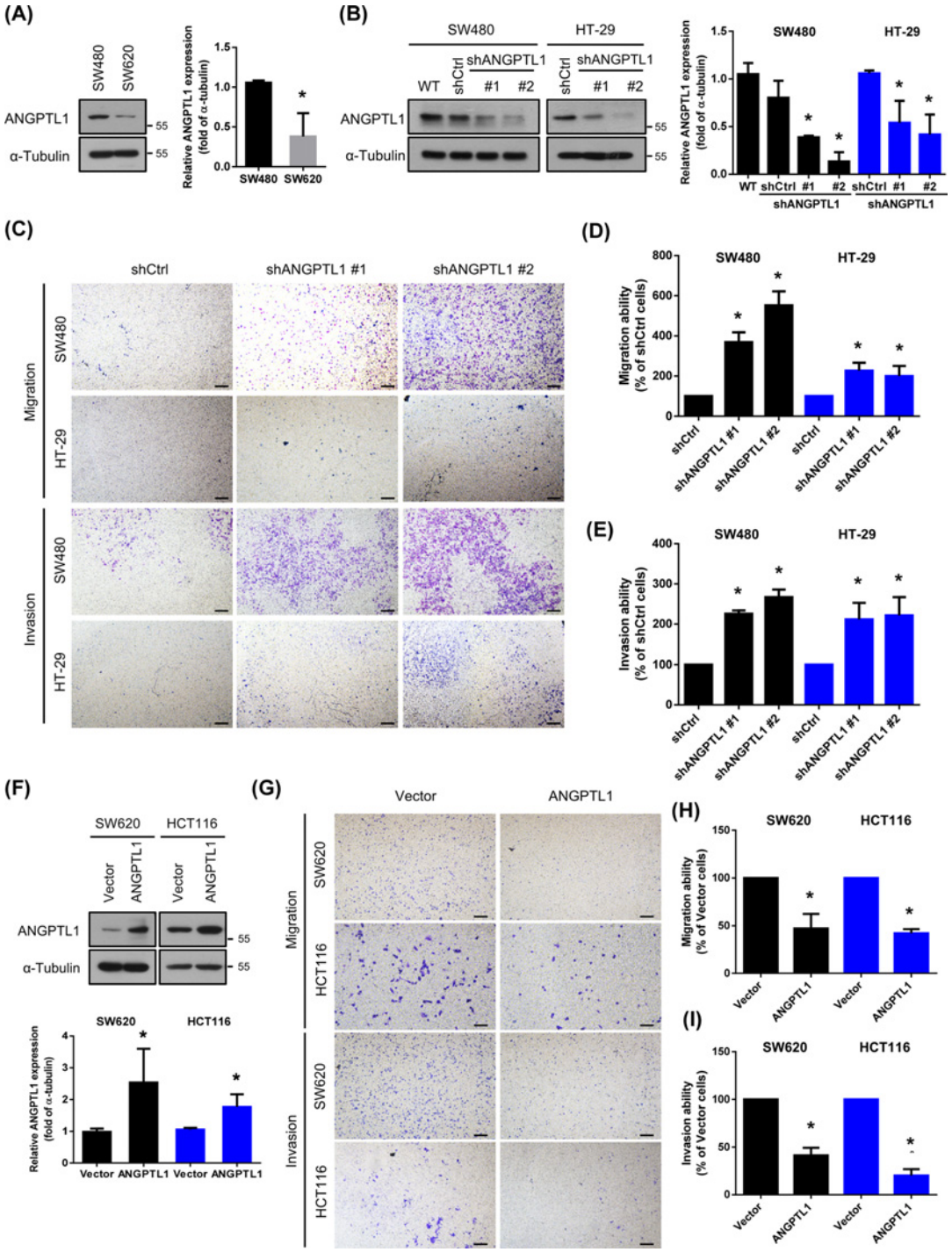

Figure 2. ANGPTL1 is required for suppression of cell mobility and metastasis in CRC

(**A**) Protein expression of ANGPTL1 in CRC cells (SW480 and the metastatic cell line SW620 cells) were analyzed by Western blotting. The expression of α-tubulin is as an internal loading control. (**B**) Knockdown efficiencies of ANGPTL1 in SW480 and HT-29 cells were analyzed by Western blotting. WT: wild-type cells; shCtrl: cells infected with scrambled shRNA virus; shANGPTL1: cells infected with shANGPTL1 virus. (**C**) Effects of ANGPTL1 inhibition on cancer cell migration and invasion for SW480 and HT-29 cells were analyzed; scale bar = 100 μm. (**D,E**) Quantification of migrated and invaded cells of ANGPTL1-silenced cells were presented as mean ± S.D. of three independent experiments. *, $P<0.05$. (**F**) Protein expression of ANGPTL1 in ANGPTL1-overexpressed SW620 and HCT116 cells was examined by Western blotting and quantified. (**G–I**) The transwell migration and invasion assays of ANGPTL1 overexpression in SW620 and HCT116 cells were determined and quantified. Results presented as the mean ± S.D. of three independent experiments. *, $P<0.05$; scale bar = 100 μm.

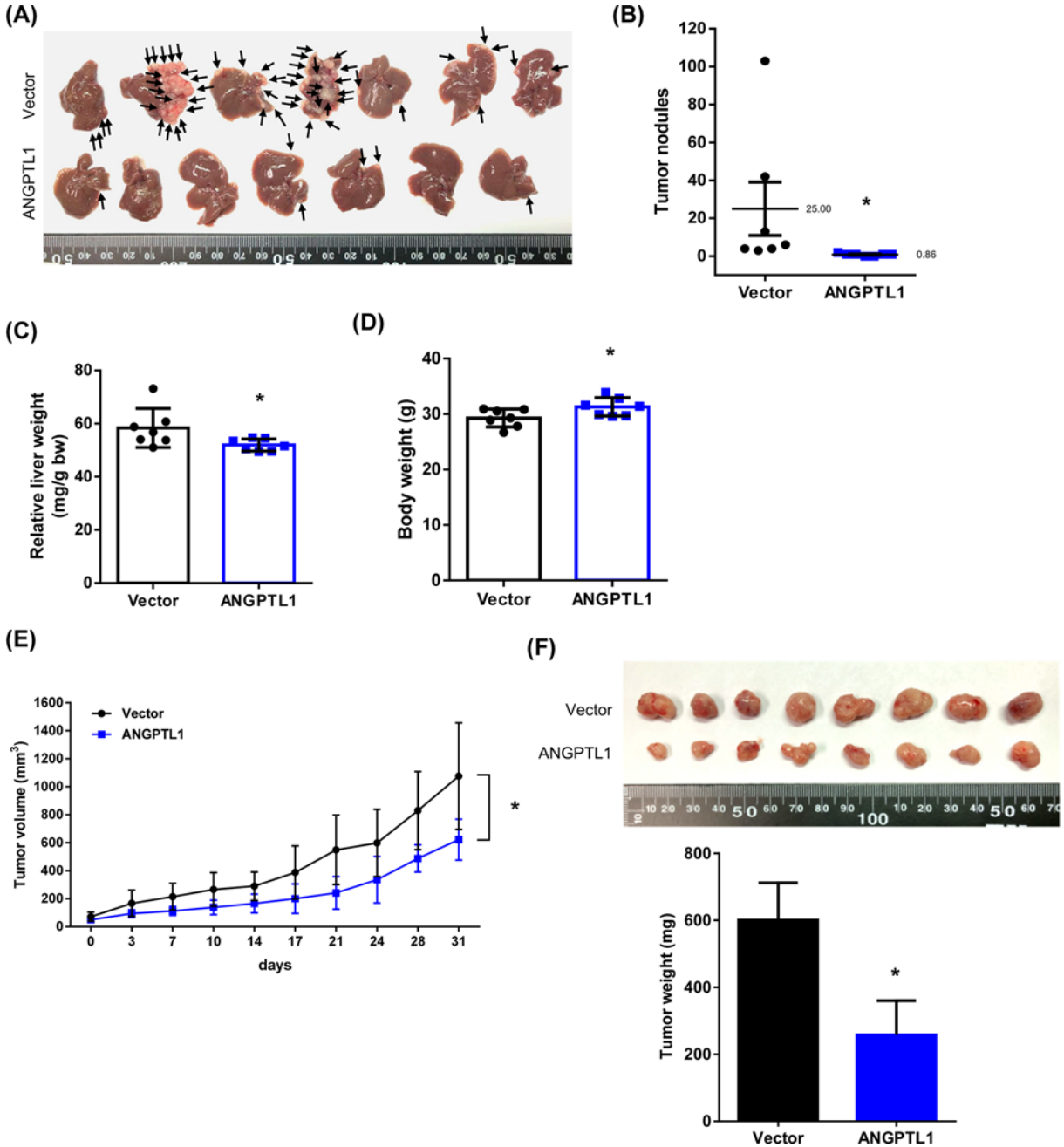

Figure 3. Effects of ANGPTL1 overexpression on liver metastasis and tumor growth in CRC

(**A**) The liver metastasis of CRC was performed with an intrasplenic injection mouse model for four weeks ($n = 7$/group). Black arrows indicated the metastatic tumor nodules in the liver. (**B**) The tumor nodules were counted and analyzed by Student's *t* test. (**C,D**) The liver and body weights were weighted; *, $P<0.05$. (**E,F**) The xenograft subcutaneous model was performed by implanted the HCT116 cells with stable expression of vector or ANGPTL1 into the dorsal flanks of nude mice. The tumor volume and tumor weight were measured. Results are represented as the mean ± S.D. *, $P<0.05$, compared with vector groups ($N = 8$/group).

(Figure 4C). The sphere formation ability and expression of CSC markers were also enhanced in the groups with ANGPTL1 silence (Figure 4D,E). Moreover, we observed that the expression levels of *ALDH1A1*, *SOX2*, *POU5F1*, and *PROM1* in colorectal cancer patients were significantly and inversely correlated with *ANGPTL1* expression from the ONCOMINE database (Table 2).

Clinical Science (2022) **136** 657–673
https://doi.org/10.1042/CS20220043

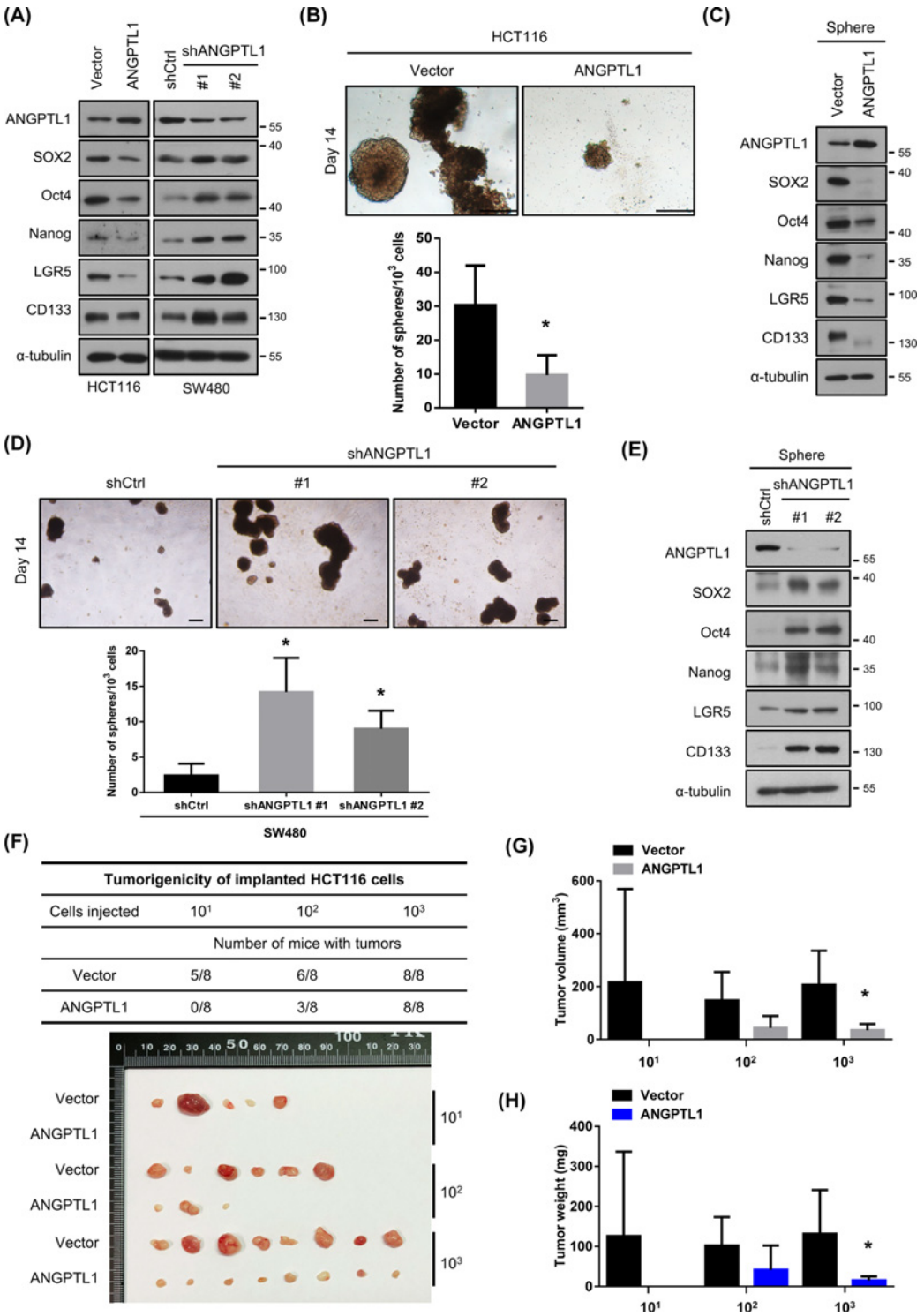

Figure 4. ANGPTL1 is critical for inhibition of cancer stem cell properties and tumorigenicity

(**A**) The protein expression of ANGPTL1 and CSC markers in CRC cells (HCT116 and SW480) were analyzed by Western blotting. The expression of α-tubulin is as an internal loading control. (**B,D**) The images of sphere formation (top) and the number of spheres in indicated cells were shown; scale bar = 100 μm. (**C,E**) The protein expression of ANGPTL1 and CSC markers in those sphere cells were assessed by Western blotting. The expression of α-tubulin is as an internal loading control. (**F–H**) The transfected cells were subcutaneously injected with indicated cell numbers (10, 100, and 1000 cells per mice) into nude mice. The tumor incidence, tumor volume, and tumor weights were analyzed. Results are shown as the mean $\pm$ S.D. *, $P<0.05$, compared with their vector control cells.

Table 2 Association between stem cell markers and *ANGPTL1* expression in colorectal cancer datasets

Stem cell markers	Datasets	Pearson correlation, r^*	*P*-value†
ALDH1A1	Tsuji (*n*=236)	−0.1806	0.0054
	Vilar (*n*=234)	−0.1883	0.0038
	Watanabe (*n*=233)	−0.1514	0.0208
SOX2	Bittner (*n*=373)	−0.1117	0.0310
	Kaiser (*n*=151)	−0.5699	<0.0001
	Skrzypczak (*n*=149)	−0.5540	<0.0001
POU5F1	Bittner (*n*=373)	−0.1585	0.0021
	Gaedcke (*n*=130)	−0.5678	<0.0001
	Hong (*n*=82)	−0.4263	<0.0001
	Kaiser (*n*=149)	−0.2560	0.0016
	TCGA (*n*=237)	−0.1335	0.0400
	Tsuji (*n*=231)	−0.2970	<0.0001
	Tsukamoto (*n*=233)	−0.2108	0.0012
	Vilar (*n*=231)	−0.2532	<0.0001
PROM1	Bittner (*n*=373)	−0.1684	0.0011
	Gaedcke (*n*=130)	−0.1784	0.0423
	Tsuji (*n*=231)	−0.4818	<0.0001
	Tsukamoto (*n*=233)	−0.4273	<0.0001
	Vilar (*n*=231)	−0.3426	<0.0001
	Watanabe (*n*=233)	−0.4129	< 0.0001

*r, Pearson's correlation coefficient.
†*P*-value for two-tailed Student's *t* test of Individual dataset (ONCOMINE database).

To further explore the tumorigenicity under the presence of ANGPTL1, subcutaneous tumorigenicity model was performed *in vivo*. The tumor incidence (number of tumors/number of implanted cells) was dramatically repressed in the group of ANGPTL1-overexpressed HCT116 cells compared with the vector group, even in the only 10 cells with ANGPTL1-overexpression group (Figure 4F). Although the tumor incidence was not changed in 1000 cells with ANGPTL1-overexpression group compared to the vector group, the tumor volume was reduced in ANGPTL1-overexpressed tumors (Figure 4G), as well as the tumor weight was significantly decreased (Figure 4H). Collectively, these results implicate that ANGPTL1 has ability to eliminate the CSC properties of CRC.

FOXO3a is involved in ANGPTL1-regulated cell mobility

It has been well known that FOXO family, including FOXO1, FOXO3a, and FOXO4, regulates cancer development, tumorigenesis, metabolism, and metastasis [23–27]. According to the potential antitumor activity of FOXO members in several cancers, we subsequently examined the expression of FOXO1, FOXO3a, and FOXO4. As shown in Figure 5A, only the expression of FOXO3a was up-regulated in ANGPTL1-overexpressed cells but not FOXO1 nor FOXO4. We further examined the mRNA expression of FOXO3a and found that the FOXO3a mRNA expression was also increased in ANGPTL1-overexpressed cells (Figure 5B). Since the transcriptional activity of FOXO3a is determined by nuclear translocation of FOXO3a, which can be inhibited with phosphorylation by kinases, the phosphorylation of FOXO3a was examined. The results showed that the FOXO3a phosphorylation was not significantly higher in ANGPTL1-overexpressed cells than vector control cells (Figure 5C, fold = 1.13; P=0.5456). Moreover, nuclear and cytosol fractions were examined to verify the nuclear translocation of FOXO3a under ANGPTL1 overexpression. The expression of FOXO3a in the nucleus was induced in ANGPTL1-overexpressed cells (Figure 5D), suggesting that ANGPTL1 not only enhanced FOXO3a mRNA expression but also nuclear translocation. To further confirm the role of FOXO3a in ANGPTL1-regulated cell mobility, the depletion of FOXO3a in ANGPTL1-overexpressed cells was examined by Western blotting (Figure 5E). FOXO3a depletion markedly abolished the ANGPTL1-reduced cell migration and invasion abilities (Figure 5F–H). These results suggest that ANGPTL1 inhibits CRC cell motility through up-regulation of FOXO3a expression.

Clinical Science (2022) **136** 657–673
https://doi.org/10.1042/CS20220043

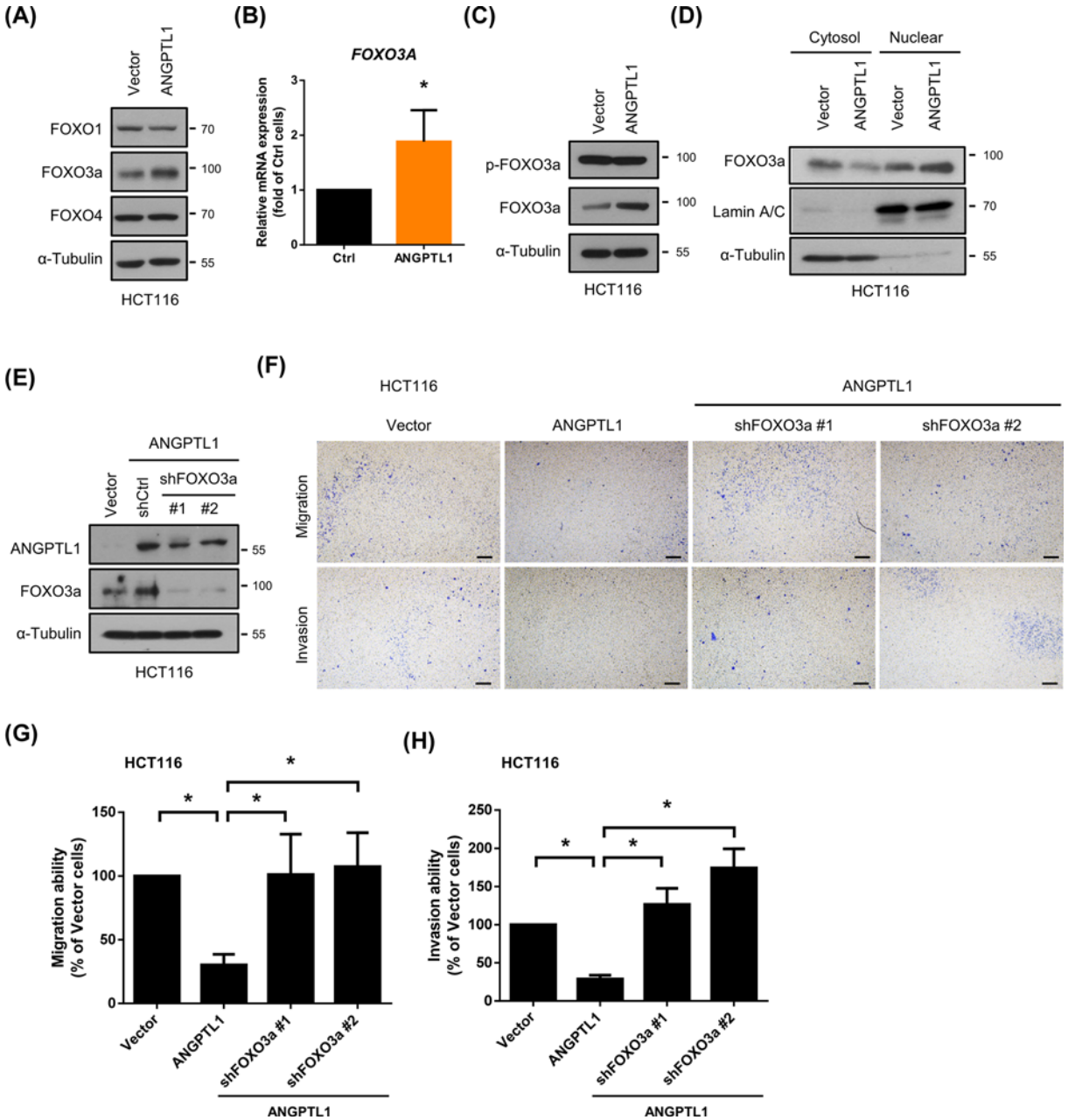

Figure 5. ANGPTL1 suppressed cell migration and invasion through FOXO3a induction in HCT116 cells

(**A**) The protein expression of FOXO family was assessed by Western blotting. The expression of α-tubulin used as an internal loading control. (**B**) The mRNA expression of FOXO3 was analyzed using RT-PCR analysis. *GAPDH* was used as reference gene; *, $P<0.05$ (**C**) The p-FOXO3a and FOXO3a expression in ANGPTL1-overexpressed cells was performed. The expression of α-tubulin is as an internal loading control. (**D**) The expression of FOXO3a in the nucleus and cytosol was assessed by Western blotting. The expression of Lamin A/C used as nuclear internal loading control and α-tubulin as a cytosol internal loading control. (**E**) The knockdown efficiencies of FOXO3a were analyzed. The expression of α-tubulin is as an internal loading control. (**F–H**) Both migration and invasion abilities were examined and quantified. Results are shown as the mean ± S.D. of three independent experiments. *, $P<0.05$, compared with indicated cells; scale bar = 100 μm.

Down-regulation of SOX2 through the ANGPTL1-up-regulated FOXO3a pathway

SOX2, a member of the SRY-related HMG-box (SOX) family, is one of the critical CSC transcription factors and directly inhibited by FOXO3a in neck squamous cell carcinoma [28]. We hypothesized that the mechanism of ANGPTL1-regulated CRC metastasis and cancer stemness may be through FOXO3a/SOX2 axis. As the results, the expression of SOX2 was reduced in ANGPTL1-overexpressed cells, while knockdown of FOXO3a restored the expression of SOX2 (Figure 6A). To further investigate the role of SOX2 in ANGPTL1/FOXO3a-suppressed metastasis and cancer stemness, we genetically silenced SOX2 using siRNA transfection. Suppression of SOX2 in ANGPTL1/shFOXO3a cells significantly reduced the sphere formation compared with the ANGPTL1/shCtrl group (Figure 6B,C), and the FOXO3a knockdown-induced cell migration and invasion abilities were also abolished (Figure 6D–F). Due to CSCs participate in tumor initiation, metastasis, drug resistance, and tumor recurrence, we investigated the effects of ANGPTL1-FOXO3a-SOX2 signaling on chemosensitivity, such as 5-fluorouracil (5-FU). We found that the inhibition of FOXO3a significantly reduced ANGPTL1-mediated sensitivity to 5-FU, but this effect was reversed by inhibition of SOX2 (Figure 6G), suggesting that ANGPTL1-FOXO3a-SOX2 signaling positively regulated the sensitization to 5-FU in colorectal cancer cells.

To further confirm the role of SOX2 in CRC stemness and metastasis, we overexpressed the expression of SOX2 in ANGPTL1/shFOXO3a/siSOX2-transfected HCT116 cells and evaluated these effects. Overexpression of SOX2 in ANGPTL1/shFOXO3a/siSOX2-transfected HCT116 cells significantly enhanced the sphere formation, and the migration/invasion abilities were also markedly restored in overexpressed SOX2 cells (Figure 7), suggesting that the expression of SOX2 played a vital role in ANGPTL1-regulated CRC stemness and metastasis. Taken together, these results suggest that ANGPTL1-up-regulated FOXO3a expression may inhibit metastasis and cancer stemness through the suppression of SOX2 in CRC cells (Figure 8).

Discussion

Accumulating studies have clarified that ANGPTL1 inhibits angiogenesis, tumor growth, and metastasis, yet the mechanisms are diverse in different cancer types, including lung cancer [29], HCC [17], and CRC [12,30]. In lung cancer, ANGPTL1 suppressed cell motility through interaction with integrin $\alpha_1\beta_1$ and reduction of Slug, then elicited mesenchymal-to-epithelial transition (MET) [29]. Another study also reported that ANGPTL1 interacted with integrin $\alpha_1\beta_1$ and repressed the Src/JAK/STAT3 signaling pathway to attenuate the HCC angiogenesis and metastasis [11]. Beside the integrin pathway, ANGPTL1 also impeded MET activation and downstream signaling, which contributed to overcome sorafenib resistance in HCC [17]. In CRC, ANGPTL1 suppressed EMT by inhibition of Slug [31] and repressed metastasis via microRNA-138 regulation [12]. A recent study has shown that exosomal ANGPTL1 retards liver metastasis using an intrasplenic injection mouse model by regulation the secretion of Kupffer cells in the liver [30]. Another study showed that intrasplenic injection of tumor cells allowed the maximum expression of the metastatic ability and disseminate to liver [32]. These studies suggested that the intrasplenic injection model could be used to investigate the role of ANGPTL1 in liver metastasis. Consistent with these previous studies, we found that ANGPTL1 suppressed CRC cell migration and invasion *in vitro*, and inhibited tumor growth and liver metastasis *in vivo*. However, in this model, CRC cells were injected into the circulation without the process of extravasation. The cecal wall injection model may be a better choice. It may be considered conducting this model for liver metastasis in the future.

During cancer initiation and metastasis, CSCs have been considered to participate in the process and modulate the tumor microenvironment. The cross-talk between endothelial cells and tumor cells or CSCs promotes EMT and angiogenesis [33,34]. A previous study has found that metastatic breast cancer cells maintain the signature of the distinct stem-like cells, including the gene expression of stem cells, EMT, survival, and dormancy [35]. The Yamanaka factors, including Sox2, Oct3/4, c-Myc, and Klf4 are established in the induced pluripotent stem (iPS) cells, leading to tumorigenesis [36,37]. Highly expression of SOX2 has been identified in CRC cells and patients, and associated with poor prognosis [38]. SOX2 promotes CSCs properties through β-catenin and transcriptional regulation of Beclin1 in CRC [39]. Inhibition of Oct4 diminished the self-renewal of colorectal cancer stem cells via EMT and positively correlated with TNM stage, lymph node metastasis and distant metastasis of CRC patients [40]. Nanog, another pluripotency-related transcription factor, has been shown to modulate the stemness [41] and facilitate the proliferation, invasion, and EMT [42] in CRC. Moreover, ANGPTL1 has been reported to inhibit the expression of CSCs markers and sphere formation by suppressing Slug in HCC [17]. However, there are no studies that have evaluated the role of ANGPTL1 in the regulation of stemness in CRC. Thus, in this study, we demonstrate that ANGPTL1 can suppress the expression of CSCs markers and sphere formation *in vitro* and tumorigenesis *in vivo* of CRC.

Clinical Science (2022) **136** 657–673
https://doi.org/10.1042/CS20220043

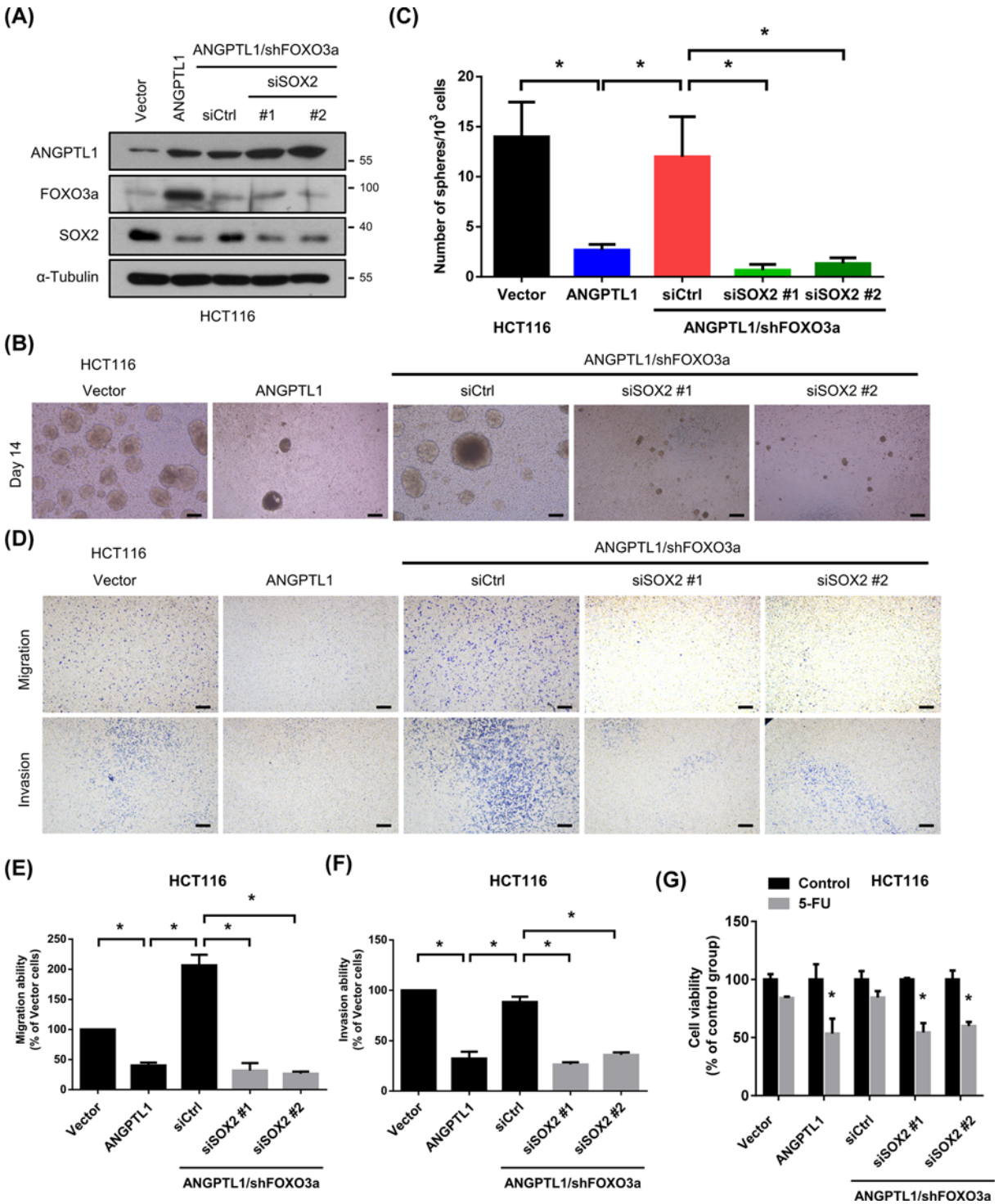

Figure 6. ANGPTL1-FOXO3a signaling pathway mediated cell motility and cancer stem cell properties via SOX2 inhibition in HCT116 cells

(**A**) The inhibition efficiencies of SOX2 by siRNA transfection were determined by Western blotting. The expression of α-tubulin is as an internal loading control. (**B,C**) The effects of SOX2 suppression on sphere formation abilities were analyzed and quantified. Bars presented as the mean ± S.D. of three independent experiments. *, $P < 0.05$, compared to indicated cells; scale bar = 100 μm. (**D–F**) The migration and invasion abilities of SOX2-silenced cells were measured in transwell assay. Results are represented as the mean ± S.D. of three independent experiments. *, $P<0.05$, compared with indicated cells; scale bar = 100 μm. (**G**) The cell viability of SOX2-silenced cells was analyzed using MTT assay after treatment with 5-FU (10 μM) for 24 h. Results are represented as the mean ± S.D. of three independent experiments. *, $P<0.05$, compared with indicated cells.

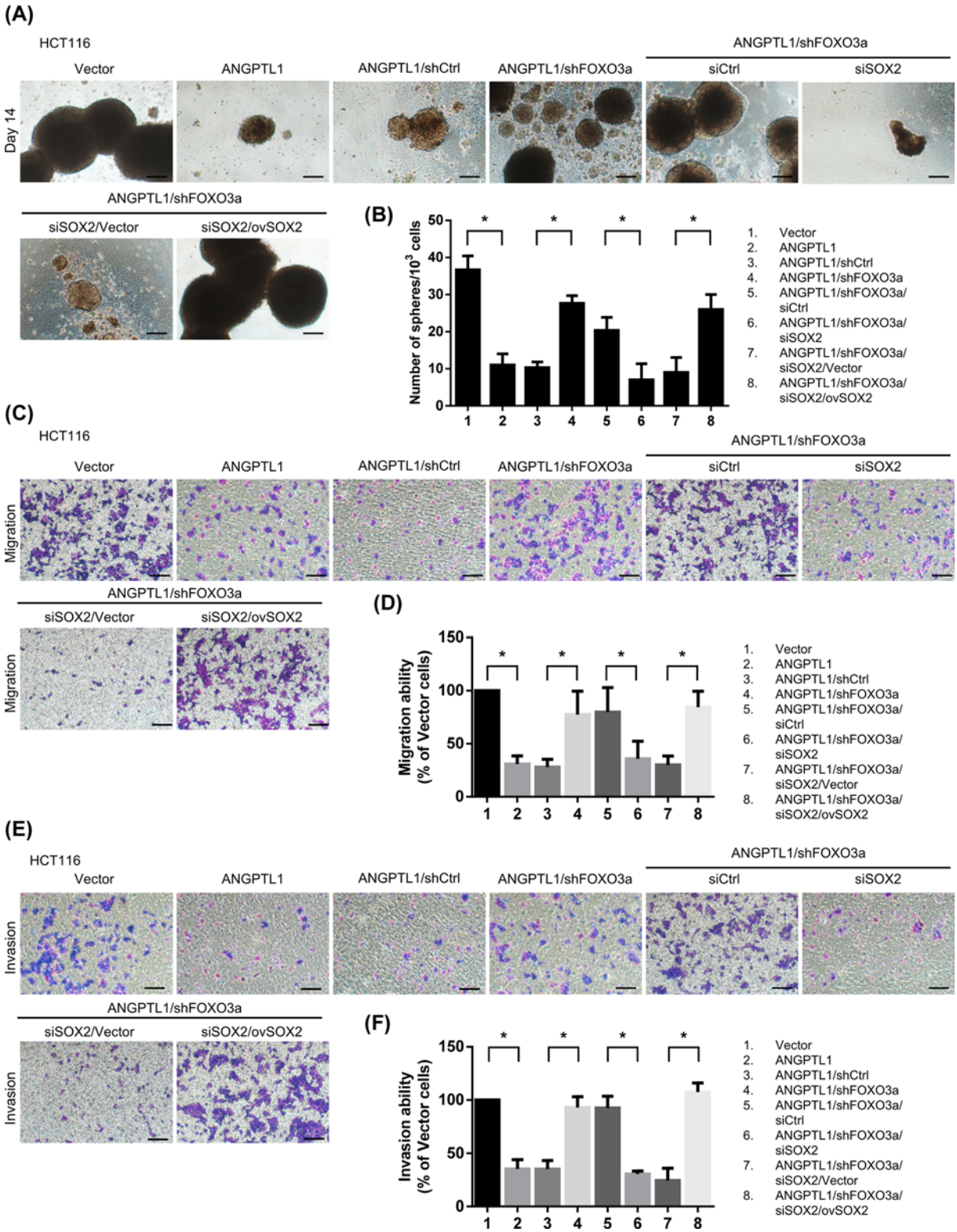

Figure 7. Restored SOX2 expression enhanced the ANGPTL1-FOXO3a-mediated cancer stemness and metastasis

(**A,B**) The sphere formation abilities in SOX2 re-overexpression were analyzed and quantified. Bars presented as the mean ± S.D. of three independent experiments. *, $P<0.05$, compared to indicated cells; scale bar: 100 μm. (**C–F**) The migration and invasion abilities of SOX2 re-overexpression in cells were measured in transwell assay. Results are represented as the mean ± S.D. of three independent experiments. *, $P<0.05$, compared with indicated cells; scale bar: 100 μm.

Clinical Science (2022) **136** 657–673
https://doi.org/10.1042/CS20220043

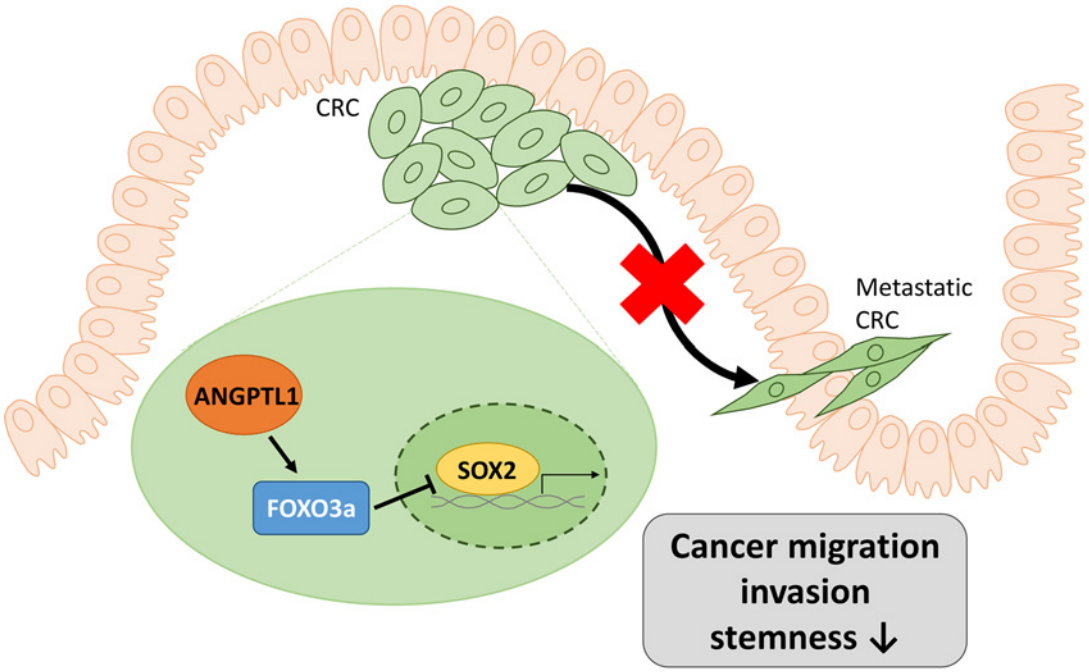

Figure 8. A schematic model illustrating the transcriptional reduction of SOX2 by ANGPTL1 through the induction of FOXO3a in CRC, and how this affects cancer stemness and metastasis

FOXO3a is a tumor suppressor and involved in the regulation of CSCs properties, metastasis, and cancer progression in various cancers [43–45]. Overexpression of FOXO3a reduced the transcriptional expression of SOX2 by directly binding on SOX2 promoter region and subsequent impeded the CSCs properties in head and neck squamous cell carcinoma [28]. In breast cancer, DNMT1 down-regulated FOXO3a expression, thereby induced the expression of FOXM1/SOX2, contributed to promote the cancer stemness and tumorigenicity [46]. In this study, our results suggest that FOXO3a drives the inhibition of SOX2 and reduction of the sphere formation and cell motility in CRC under ANGPTL1 regulation. We also found that ANGPTL1 not only enhanced FOXO3a mRNA expression but also triggered the nuclear translocation of FOXO3a. These findings can also help for completing the knowledge of FOXO3a in cancer stemness in various types of cancers. However, the detailed mechanism for ANGPTL1-regulated FOXO3a expression still needs to be further investigation in future research.

Conclusion

Our findings uncover a novel mechanism of ANGPTL1/FOXO3a/SOX2 axis that suppresses cancer migration, invasion, and stemness in CRC. We also demonstrate the clinical significance of ANGPTL1 that there is a clinically inverse association between CSCs markers and *ANGPTL1* in CRC patients. These results figure out the important roles of ANGPTL1 in the CRC stemness and progression and may provide a potential target to develop therapeutic strategies or novel prognosis markers for colorectal cancer patients. However, the limitation of this study is lack of the evidence of ANGPTL1-FOXO3a-SOX2-mediated cancer stemness in animal model. It may be possible in the future to analyze the *in vivo* ANGPTL1-FOXO3a-SOX2-mediated cancer stemness.

Clinical perspectives

- Previous studies have shown that ANGPTL1 plays a crucial role in cancer progression by suppressing cancer cell proliferation and motility in various cancers. However, there may have undefined functions and molecular mechanisms involved in the tumor progression mediated by ANGPTL1. Thus, this

study was aimed to identify the role of ANGPTL1 in metastasis, cancer stemness, and the molecular mechanisms of colorectal cancer.

- We found for the first time that ANGPTL1 significantly suppressed the cancer migration, invasion, and stemness by enhancing FOXO3a expression, which reduced the stem cell transcription factor SOX2 expression in CRC.
- This study demonstrates the detail molecular mechanism of ANGPTL1 suppresses cancer migration, invasion, and stemness in colorectal cancer cells. Furthermore, define the biological significance of ANGPTL1 may provide more potential targets to develop the anticancer therapeutic strategies or novel prognosis markers for colorectal cancer patients.

Data Availability

The data presented in this study are available from the corresponding author upon reasonable request. The full uncropped and unedited versions of the representative Western blot images are listed in the Supplementary Figure.

Competing Interests

The authors declare that there are no competing interests associated with the manuscript.

Funding

This study was funded in part by grants from the Ministry of Science and Technology of Taiwan [grant numbers MOST-106-2320-B-005-001-MY3; MOST107-2314-B-002-251] and the Teh-Tzer Study Group for Human Medical Research Foundation [grant numbers B1081007 and B1101008].

CRediT Author Contribution

Ting-Yu Chang: Data curation, Formal analysis, Validation, Investigation, Visualization, Methodology, and Writing—original draft. **Kuo-Cheng Lan:** Resources, Funding acquisition, Validation, and Writing—review & editing. **Chen-Yuan Chiu:** Resources, Funding acquisition, and Validation. **Meei-Ling Sheu:** Resources, Supervision, Funding acquisition, Validation, and Writing—review & editing. **Shing-Hwa Liu:** Resources, Supervision, Funding acquisition, Validation, and Writing—review & editing.

Acknowledgements

We thank the National RNAi Core Facility (Academia Sinica, Taipei, Taiwan) for providing specific shRNAs and the results shown here are in part based on data generated from the ONCOMINE database.

Abbreviations

ANGPTL1, angiopoietin-like protein 1; CRC, colorectal cancer; CSC, cancer stem cell; EMT, epithelial–mesenchymal transition; FBS, fetal bovine serum; FOXO3a, forkhead box O-3a; IHC, immunohistochemistry; shRNA, short hairpin RNA; siRNA, small interfering RNA; SOX2, SRY-related HMG-box-2; TMA, tissue microarrays.

References

1 Siegel, R.L., Miller, K.D., Fuchs, H.E. and Jemal, A. (2022) Cancer statistics, 2022. *CA Cancer J. Clin.* **72**, 7–33, https://doi.org/10.3322/caac.21708
2 Gonzalez-Villarreal, C.A., Quiroz-Reyes, A.G., Islas, J.F. and Garza-Trevino, E.N. (2020) Colorectal cancer stem cells in the progression to liver metastasis. *Front. Oncol.* **10**, 1511, https://doi.org/10.3389/fonc.2020.01511
3 Mani, S.A., Guo, W., Liao, M.J., Eaton, E.N., Ayyanan, A., Zhou, A.Y. et al. (2008) The epithelial-mesenchymal transition generates cells with properties of stem cells. *Cell* **133**, 704–715, https://doi.org/10.1016/j.cell.2008.03.027
4 Diehn, M., Cho, R.W., Lobo, N.A., Kalisky, T., Dorie, M.J., Kulp, A.N. et al. (2009) Association of reactive oxygen species levels and radioresistance in cancer stem cells. *Nature* **458**, 780–783, https://doi.org/10.1038/nature07733
5 Phi, L.T.H., Sari, I.N., Yang, Y.G., Lee, S.H., Jun, N., Kim, K.S. et al. (2018) Cancer stem cells (CSCs) in drug resistance and their therapeutic implications in cancer treatment. *Stem. Cell Int.* **2018**, 5416923, https://doi.org/10.1155/2018/5416923
6 Quante, M., Tu, S.P., Tomita, H., Gonda, T., Wang, S.S., Takashi, S. et al. (2011) Bone marrow-derived myofibroblasts contribute to the mesenchymal stem cell niche and promote tumor growth. *Cancer Cell* **19**, 257–272, https://doi.org/10.1016/j.ccr.2011.01.020
7 Fumagalli, A., Oost, K.C., Kester, L., Morgner, J., Bornes, L., Bruens, L. et al. (2020) Plasticity of Lgr5-negative cancer cells drives metastasis in colorectal cancer. *Cell Stem Cell* **26**, 569.e7–578.e7, https://doi.org/10.1016/j.stem.2020.02.008

8 Frank, M.H., Wilson, B.J., Gold, J.S. and Frank, N.Y. (2021) Clinical implications of colorectal cancer stem cells in the age of single-cell omics and targeted therapies. *Gastroenterology* **160**, 1947–1960, https://doi.org/10.1053/j.gastro.2020.12.080
9 Kuo, T.C., Tan, C.T., Chang, Y.W., Hong, C.C., Lee, W.J., Chen, M.W. et al. (2017) Angiopoietin-like protein 1 suppresses SLUG to inhibit cancer cell motility. *J. Clin. Invest.* **127**, 402, https://doi.org/10.1172/JCI91882
10 Sun, R., Yang, L., Hu, Y., Wang, Y., Zhang, Q., Zhang, Y. et al. (2020) ANGPTL1 is a potential biomarker for differentiated thyroid cancer diagnosis and recurrence. *Oncol. Lett.* **20**, 240, https://doi.org/10.3892/ol.2020.12103
11 Yan, Q., Jiang, L., Liu, M., Yu, D., Zhang, Y., Li, Y. et al. (2017) ANGPTL1 interacts with integrin alpha1beta1 to suppress HCC angiogenesis and metastasis by inhibiting JAK2/STAT3 signaling. *Cancer Res.* **77**, 5831–5845, https://doi.org/10.1158/0008-5472.CAN-17-0579
12 Chen, H., Xiao, Q., Hu, Y., Chen, L., Jiang, K., Tang, Y. et al. (2017) ANGPTL1 attenuates colorectal cancer metastasis by up-regulating microRNA-138. *J. Exp. Clin. Cancer Res.* **36**, 78, https://doi.org/10.1186/s13046-017-0548-7
13 Xu, Y., Liu, Y.J. and Yu, Q. (2004) Angiopoietin-3 inhibits pulmonary metastasis by inhibiting tumor angiogenesis. *Cancer Res.* **64**, 6119–6126, https://doi.org/10.1158/0008-5472.CAN-04-1054
14 Carbone, C., Piro, G., Merz, V., Simionato, F., Santoro, R., Zecchetto, C. et al. (2018) Angiopoietin-like proteins in angiogenesis, inflammation and cancer. *Int. J. Mol. Sci.* **19**, 431, https://doi.org/10.3390/ijms19020431
15 Zhang, C.C., Kaba, M., Ge, G., Xie, K., Tong, W., Hug, C. et al. (2006) Angiopoietin-like proteins stimulate ex vivo expansion of hematopoietic stem cells. *Nat. Med.* **12**, 240–245, https://doi.org/10.1038/nm1342
16 Kersten, S. (2005) Regulation of lipid metabolism via angiopoietin-like proteins. *Biochem. Soc. Trans.* **33**, 1059–1062, https://doi.org/10.1042/BST0331059
17 Chen, H.A., Kuo, T.C., Tseng, C.F., Ma, J.T., Yang, S.T., Yen, C.J. et al. (2016) Angiopoietin-like protein 1 antagonizes MET receptor activity to repress sorafenib resistance and cancer stemness in hepatocellular carcinoma. *Hepatology* **64**, 1637–1651, https://doi.org/10.1002/hep.28773
18 Endo, M. (2019) The roles of ANGPTL families in cancer progression. *J. UOEH* **41**, 317–325, https://doi.org/10.7888/juoeh.41.317
19 Varghese, F., Bukhari, A.B., Malhotra, R. and De, A. (2014) IHC Profiler: an open source plugin for the quantitative evaluation and automated scoring of immunohistochemistry images of human tissue samples. *PLoS ONE* **9**, e96801, https://doi.org/10.1371/journal.pone.0096801
20 Chang, T.Y., Wu, C.T., Sheu, M.L., Yang, R.S. and Liu, S.H. (2021) CARMA3 promotes colorectal cancer cell motility and cancer stemness via YAP-mediated NF-κB activation. *Cancers* **13**, 5946, https://doi.org/10.3390/cancers13235946
21 Hewitt, R.E., McMarlin, A., Kleiner, D., Wersto, R., Martin, P., Tsokos, M. et al. (2000) Validation of a model of colon cancer progression. *J. Pathol.* **192**, 446–454, https://doi.org/10.1002/1096-9896(2000)9999:9999%3c::AID-PATH775%3e3.0.CO;2-K
22 Dafflon, C., Santamaría-Martínez, A. and Ordóñez-Morán, P. (2020) An intrasplenic injection model for the study of cancer stem cell seeding capacity. *Method. Mol. Biol. (Clifton, N.J.)* **2171**, 293–302, https://doi.org/10.1007/978-1-0716-0747-3˙20
23 Pan, S., Deng, Y., Fu, J., Zhang, Y., Zhang, Z., Ru, X. et al. (2018) Decreased expression of ARHGAP15 promotes the development of colorectal cancer through PTEN/AKT/FOXO1 axis. *Cell Death Dis.* **9**, 673, https://doi.org/10.1038/s41419-018-0707-6
24 Bullock, M.D., Bruce, A., Sreekumar, R., Curtis, N., Cheung, T., Reading, I. et al. (2013) FOXO3 expression during colorectal cancer progression: biomarker potential reflects a tumour suppressor role. *Br. J. Cancer* **109**, 387–394, https://doi.org/10.1038/bjc.2013.355
25 Liu, L., Yan, X., Wu, D., Yang, Y., Li, M., Su, Y. et al. (2018) High expression of Ras-related protein 1A promotes an aggressive phenotype in colorectal cancer via PTEN/FOXO3/CCND1 pathway. *J. Exp. Clin. Cancer Res.* **37**, 178, https://doi.org/10.1186/s13046-018-0827-y
26 Liu, X., Zhang, Z., Sun, L., Chai, N., Tang, S., Jin, J. et al. (2011) MicroRNA-499-5p promotes cellular invasion and tumor metastasis in colorectal cancer by targeting FOXO4 and PDCD4. *Carcinogenesis* **32**, 1798–1805, https://doi.org/10.1093/carcin/bgr213
27 Sun, Y., Wang, L., Xu, X., Han, P., Wu, J., Tian, X. et al. (2021) FOXO4 inhibits the migration and metastasis of colorectal cancer by regulating the APC2/beta-Catenin axis. *Front. Cell. Dev. Biol.* **9**, 659731, https://doi.org/10.3389/fcell.2021.659731
28 Chen, Y., Zhao, H., Liang, W., Jiang, E., Zhou, X., Shao, Z. et al. (2022) Autophagy regulates the cancer stem cell phenotype of head and neck squamous cell carcinoma through the noncanonical FOXO3/SOX2 axis. *Oncogene* **41**, 634–646, https://doi.org/10.1038/s41388-021-02115-7
29 Kuo, T.C., Tan, C.T., Chang, Y.W., Hong, C.C., Lee, W.J., Chen, M.W. et al. (2013) Angiopoietin-like protein 1 suppresses SLUG to inhibit cancer cell motility. *J. Clin. Invest.* **123**, 1082–1095, https://doi.org/10.1172/JCI64044
30 Jiang, K., Chen, H., Fang, Y., Chen, L., Zhong, C., Bu, T. et al. (2021) Exosomal ANGPTL1 attenuates colorectal cancer liver metastasis by regulating Kupffer cell secretion pattern and impeding MMP9 induced vascular leakiness. *J. Exp. Clin. Cancer Res.* **40**, 21, https://doi.org/10.1186/s13046-020-01816-3
31 Fan, H., Huang, L., Zhuang, X., Ai, F. and Sun, W. (2019) Angiopoietin-like protein 1 inhibits epithelial to mesenchymal transition in colorectal cancer cells via suppress Slug expression. *Cytotechnology* **71**, 35–44, https://doi.org/10.1007/s10616-018-0259-8
32 Kozlowski, J.M., Fidler, I.J., Campbell, D., Xu, Z.L., Kaighn, M.E. and Hart, I.R. (1984) Metastatic behavior of human tumor cell lines grown in the nude mouse. *Cancer Res. 44* **8**, 3522–3529
33 Galan-Moya, E.M., Le Guelte, A., Lima Fernandes, E., Thirant, C., Dwyer, J., Bidere, N. et al. (2011) Secreted factors from brain endothelial cells maintain glioblastoma stem-like cell expansion through the mTOR pathway. *EMBO Rep.* **12**, 470–476, https://doi.org/10.1038/embor.2011.39
34 Lu, J., Ye, X., Fan, F., Xia, L., Bhattacharya, R., Bellister, S. et al. (2013) Endothelial cells promote the colorectal cancer stem cell phenotype through a soluble form of Jagged-1. *Cancer Cell* **23**, 171–185, https://doi.org/10.1016/j.ccr.2012.12.021
35 Minn, A.J., Gupta, G.P., Siegel, P.M., Bos, P.D., Shu, W., Giri, D.D. et al. (2005) Genes that mediate breast cancer metastasis to lung. *Nature* **436**, 518–524, https://doi.org/10.1038/nature03799
36 Takahashi, K. and Yamanaka, S. (2006) Induction of pluripotent stem cells from mouse embryonic and adult fibroblast cultures by defined factors. *Cell* **126**, 663–676, https://doi.org/10.1016/j.cell.2006.07.024
37 Ohnishi, K., Semi, K., Yamamoto, T., Shimizu, M., Tanaka, A., Mitsunaga, K. et al. (2014) Premature termination of reprogramming in vivo leads to cancer development through altered epigenetic regulation. *Cell* **156**, 663–677, https://doi.org/10.1016/j.cell.2014.01.005

38 Takeda, K., Mizushima, T., Yokoyama, Y., Hirose, H., Wu, X., Qian, Y. et al. (2018) Sox2 is associated with cancer stem-like properties in colorectal cancer. *Sci. Rep.* **8**, 17639, https://doi.org/10.1038/s41598-018-36251-0
39 Zhu, Y., Huang, S., Chen, S., Chen, J., Wang, Z., Wang, Y. et al. (2021) SOX2 promotes chemoresistance, cancer stem cells properties, and epithelial-mesenchymal transition by beta-catenin and Beclin1/autophagy signaling in colorectal cancer. *Cell Death Dis.* **12**, 449, https://doi.org/10.1038/s41419-021-03733-5
40 Zhou, J.M., Hu, S.Q., Jiang, H., Chen, Y.L., Feng, J.H., Chen, Z.Q. et al. (2019) OCT4B1 Promoted EMT and Regulated the Self-Renewal of CSCs in CRC: Effects Associated with the Balance of miR-8064/PLK1. *Mol. Ther. Oncolytics* **15**, 7–20, https://doi.org/10.1016/j.omto.2019.08.004
41 Zhang, J., Espinoza, L.A., Kinders, R.J., Lawrence, S.M., Pfister, T.D., Zhou, M. et al. (2013) NANOG modulates stemness in human colorectal cancer. *Oncogene* **32**, 4397–4405, https://doi.org/10.1038/onc.2012.461
42 Meng, H.M., Zheng, P., Wang, X.Y., Liu, C., Sui, H.M., Wu, S.J. et al. (2010) Over-expression of Nanog predicts tumor progression and poor prognosis in colorectal cancer. *Cancer Biol. Ther.* **9**, 295–302, https://doi.org/10.4161/cbt.9.4.10666
43 Smit, L., Berns, K., Spence, K., Ryder, W.D., Zeps, N., Madiredjo, M. et al. (2016) An integrated genomic approach identifies that the PI3K/AKT/FOXO pathway is involved in breast cancer tumor initiation. *Oncotarget* **7**, 2596–2610, https://doi.org/10.18632/oncotarget.6354
44 Prabhu, V.V., Allen, J.E., Dicker, D.T. and El-Deiry, W.S. (2015) Small-molecule ONC201/TIC10 targets chemotherapy-resistant colorectal cancer stem-like cells in an Akt/Foxo3a/TRAIL-dependent manner. *Cancer Res.* **75**, 1423–1432, https://doi.org/10.1158/0008-5472.CAN-13-3451
45 Chiu, C.F., Chang, Y.W., Kuo, K.T., Shen, Y.S., Liu, C.Y., Yu, Y.H. et al. (2016) NF-kappaB-driven suppression of FOXO3a contributes to EGFR mutation-independent gefitinib resistance. *Proc. Natl. Acad. Sci. U.S.A.* **113**, E2526–E2535, https://doi.org/10.1073/pnas.1522612113
46 Liu, H., Song, Y., Qiu, H., Liu, Y., Luo, K., Yi, Y. et al. (2020) Downregulation of FOXO3a by DNMT1 promotes breast cancer stem cell properties and tumorigenesis. *Cell Death Differ.* **27**, 966–983, https://doi.org/10.1038/s41418-019-0389-3

Supplementary Information

ANGPTL1 attenuates cancer migration, invasion, and stemness through regulating FOXO3a-mediated SOX2 expression in colorectal cancer

Ting-Yu Chang, Kuo-Cheng Lan, Chen-Yuan Chiu, Meei-Ling Sheu, Shing-Hwa Liu

Western blot raw data

1. Figure 2A

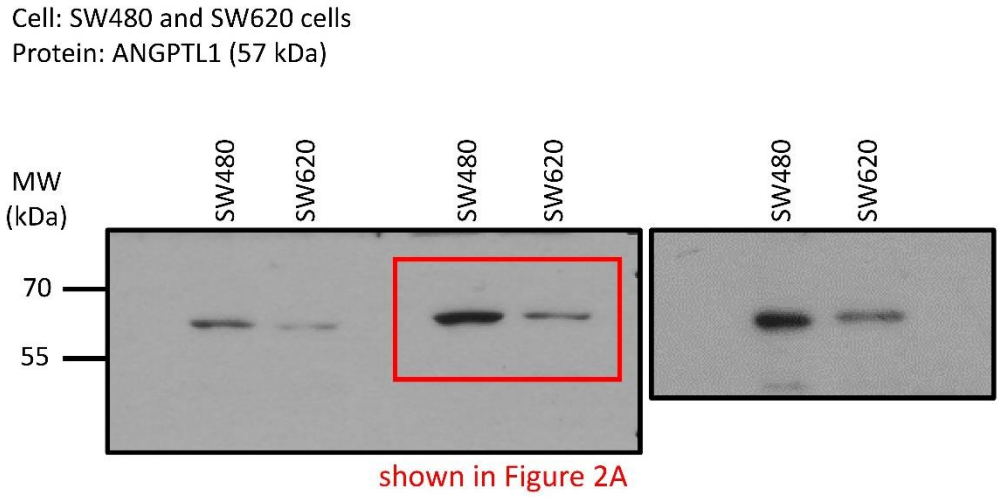

2. Figure 2A

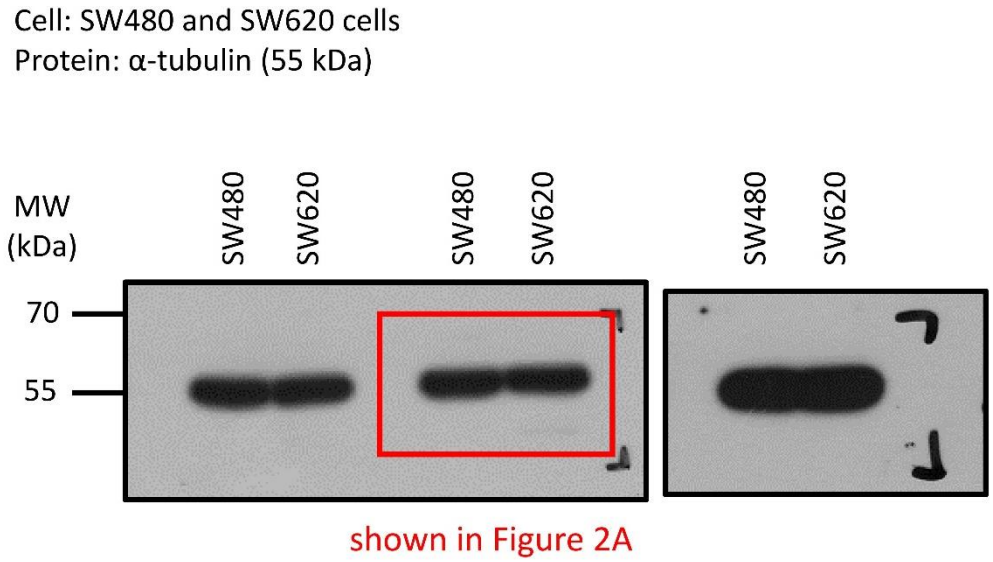

3. Figure 2B-left

Cell: SW480 cells
Protein: ANGPTL1 (57 kDa)

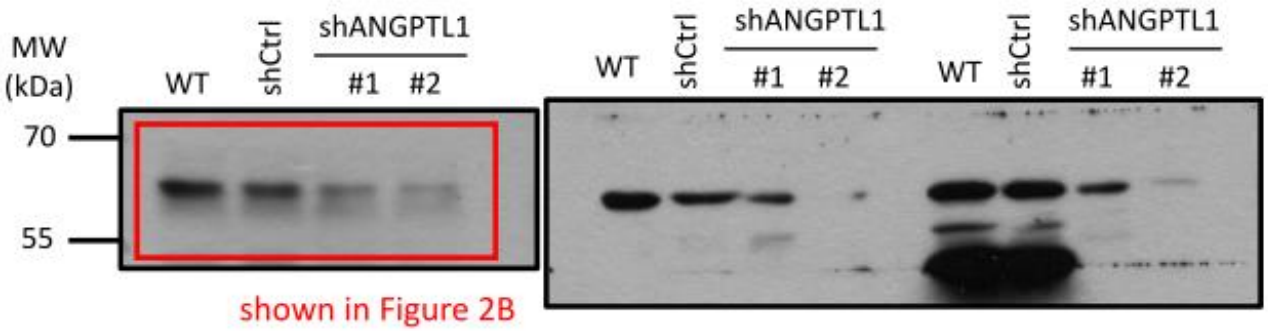

4. Figure 2B-left

Cell: SW480 cells
Protein: α-tubulin (55 kDa)

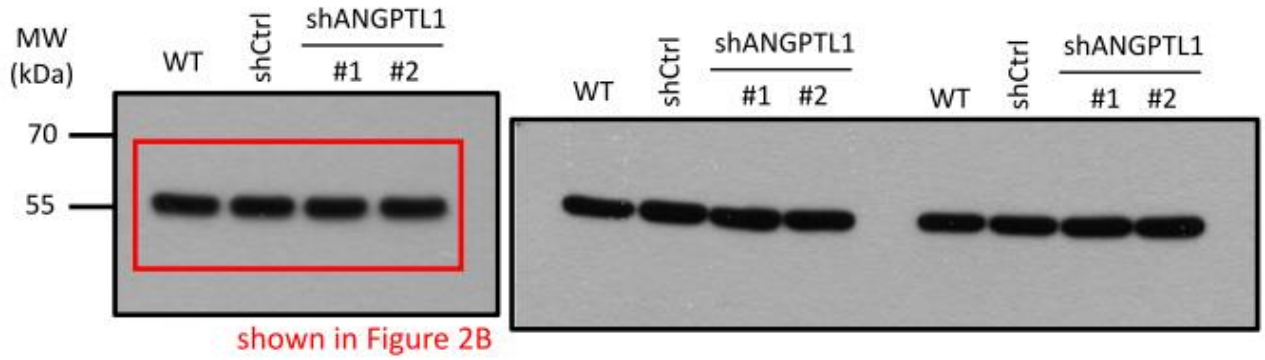

5. Figure 2B-right

Cell: HT-29 cells
Protein: ANGPTL1 (57 kDa)

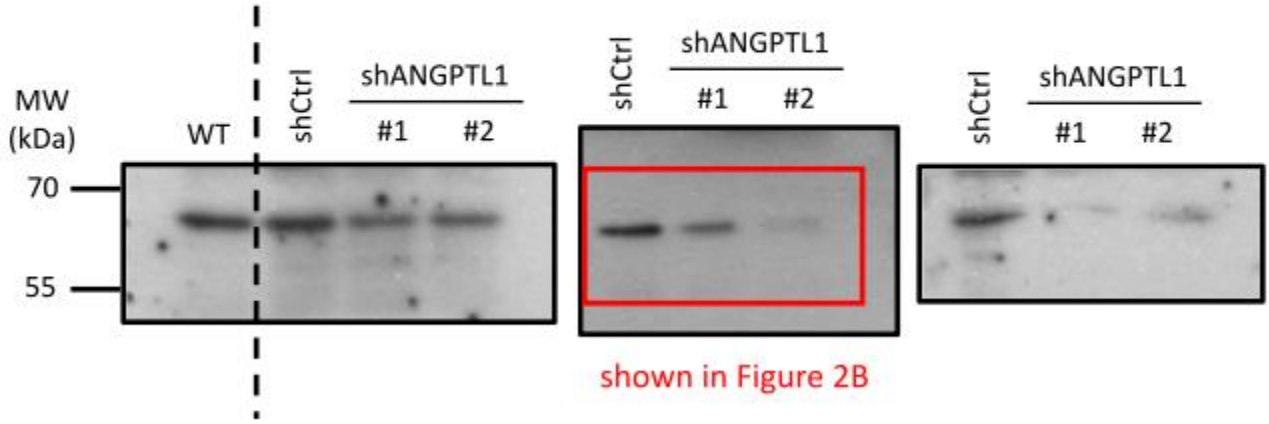

6. Figure 2B-right

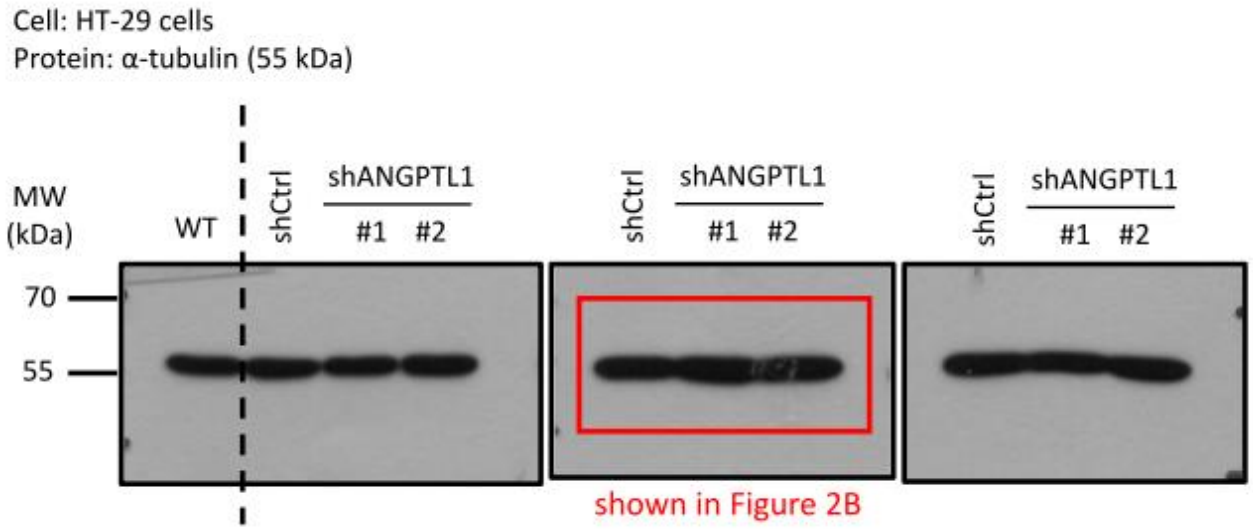

7. Figure 2F-left

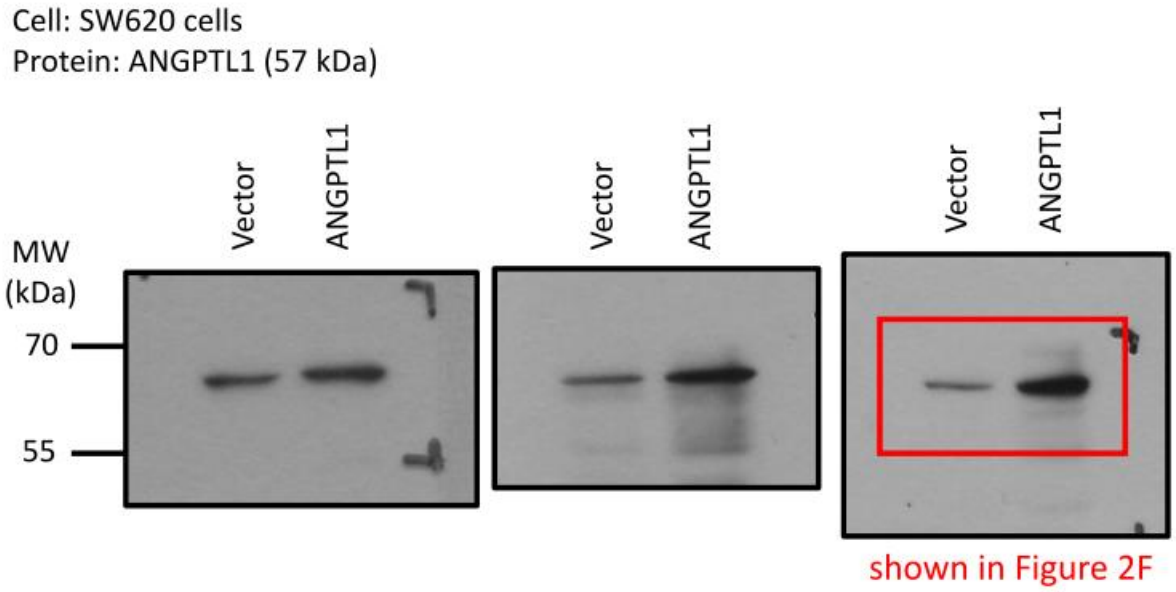

8. Figure 2F-left

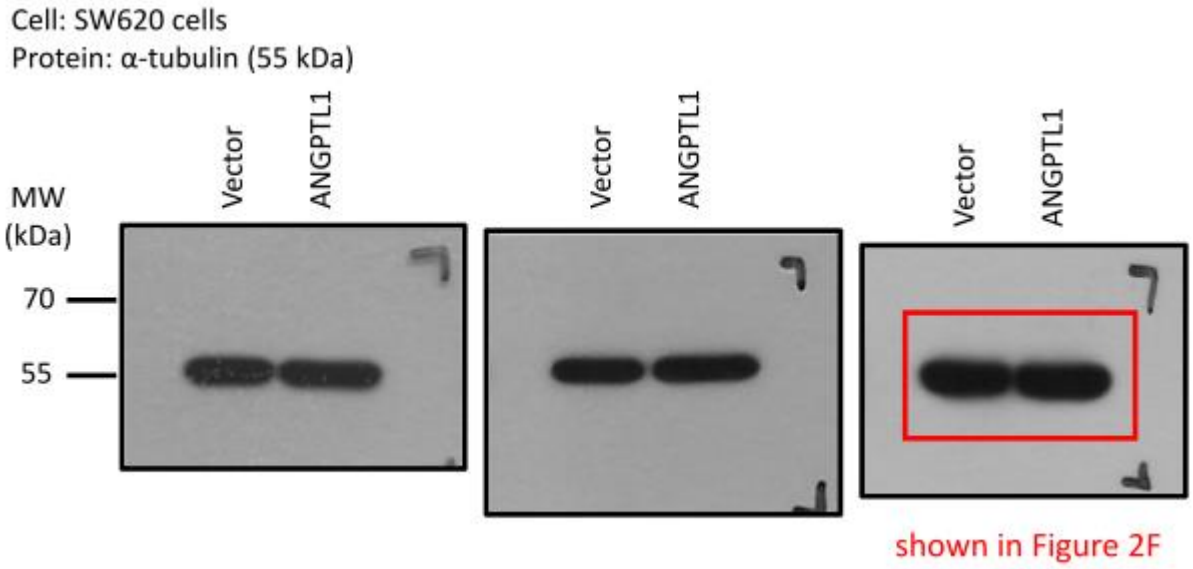

9. Figure 2F-right

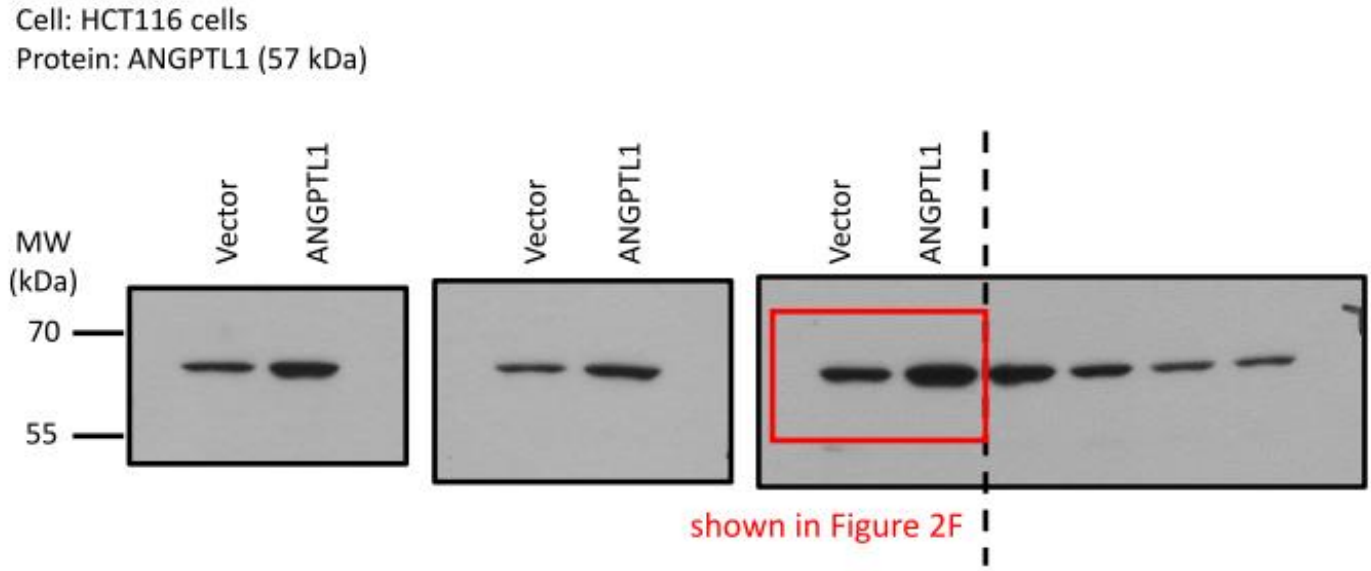

10. Figure 2F-right

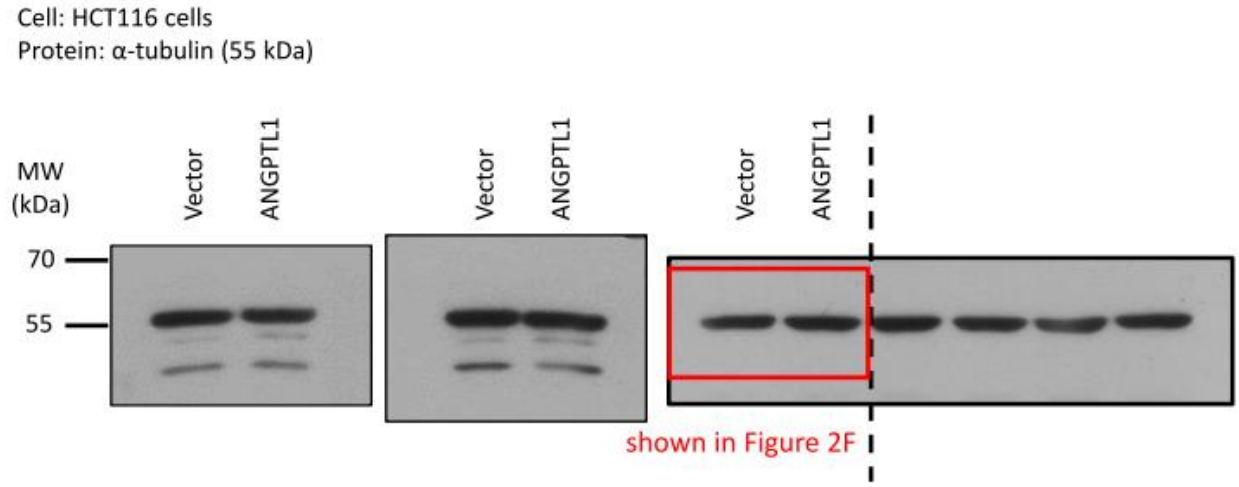

11. Figure 4A-left

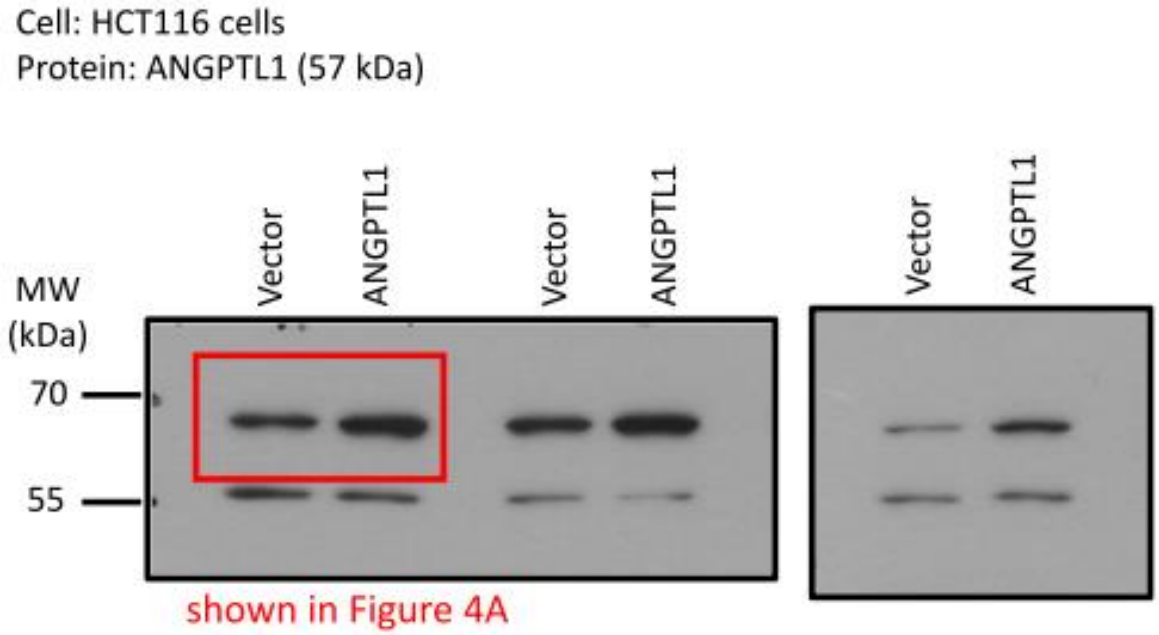

12. Figure 4A-left

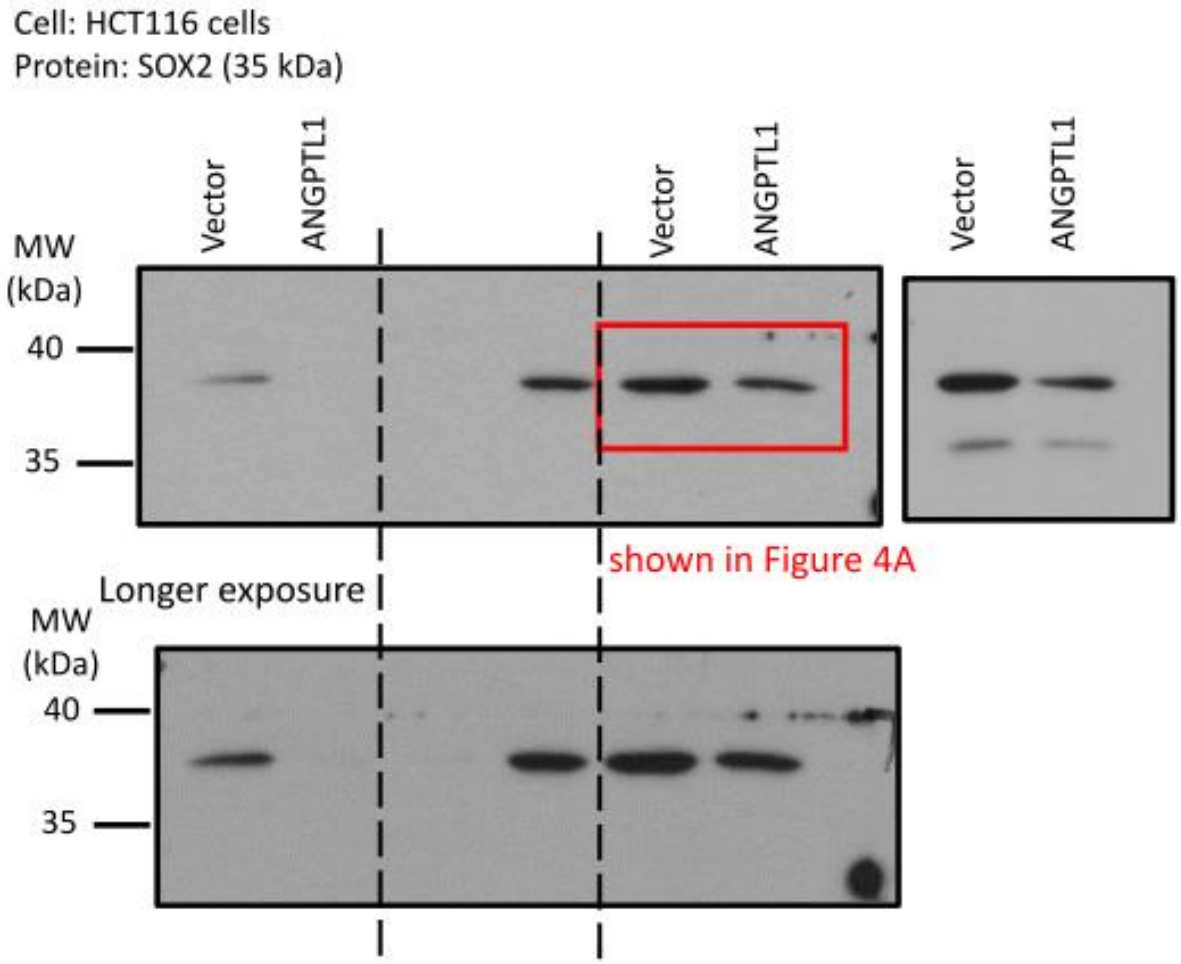

13. Figure 4A-left

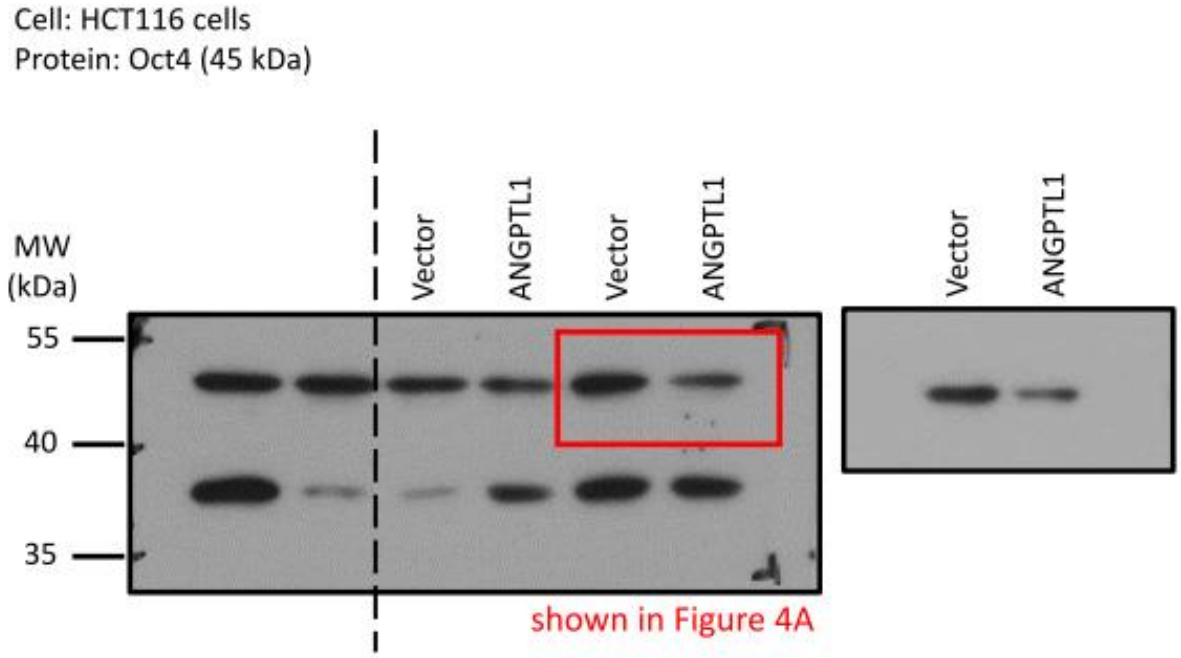

14. Figure 4A-left

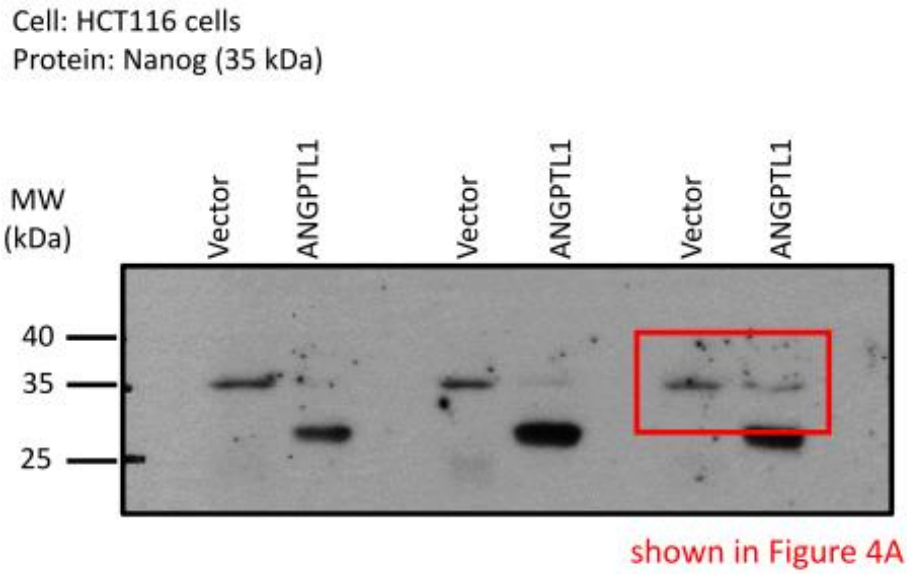

15. Figure 5A-left

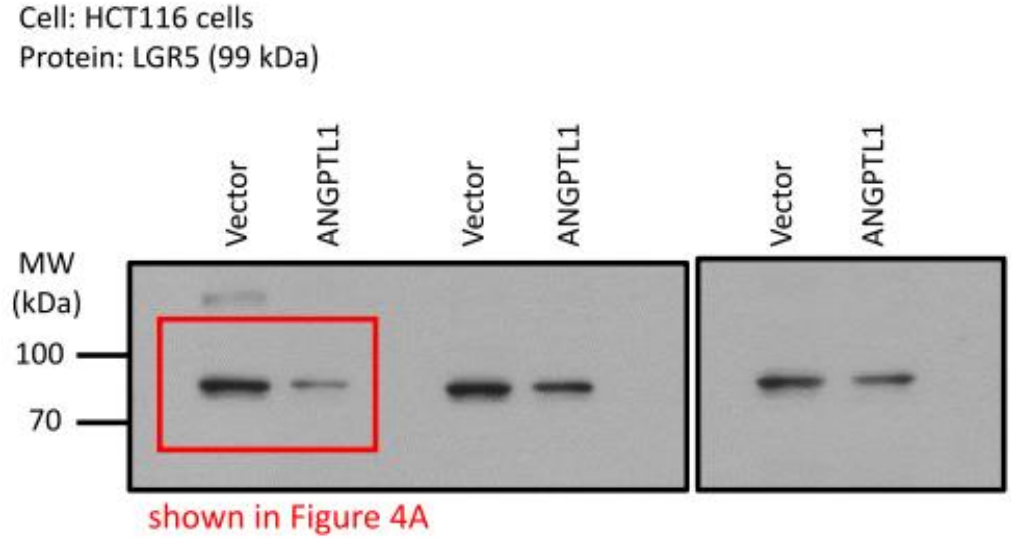

16. Figure 4A-left

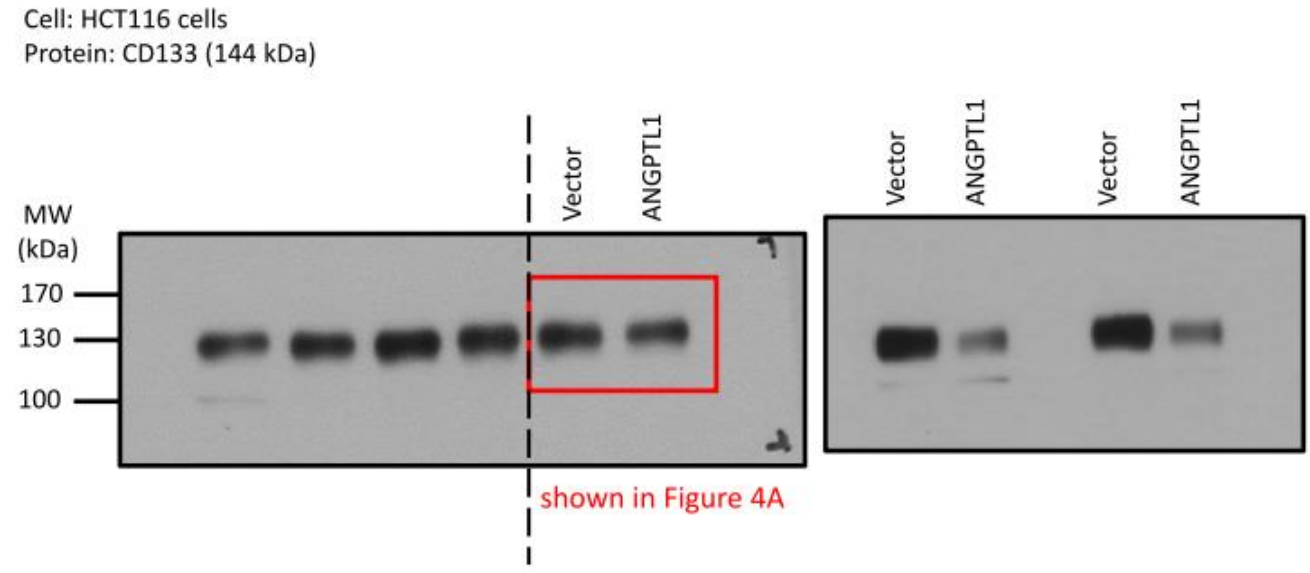

17. Figure 4A-left

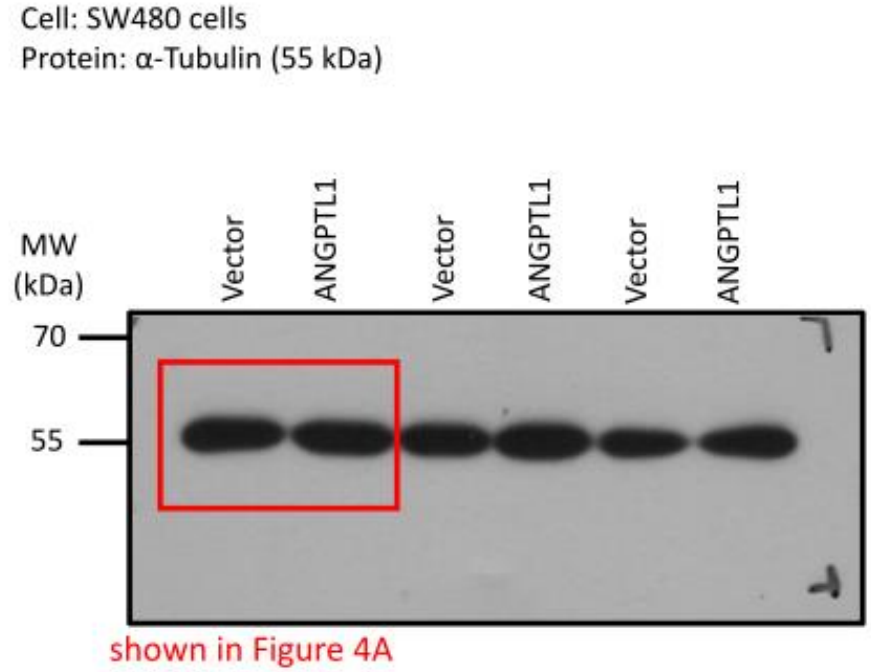

18. Figure 4A-right

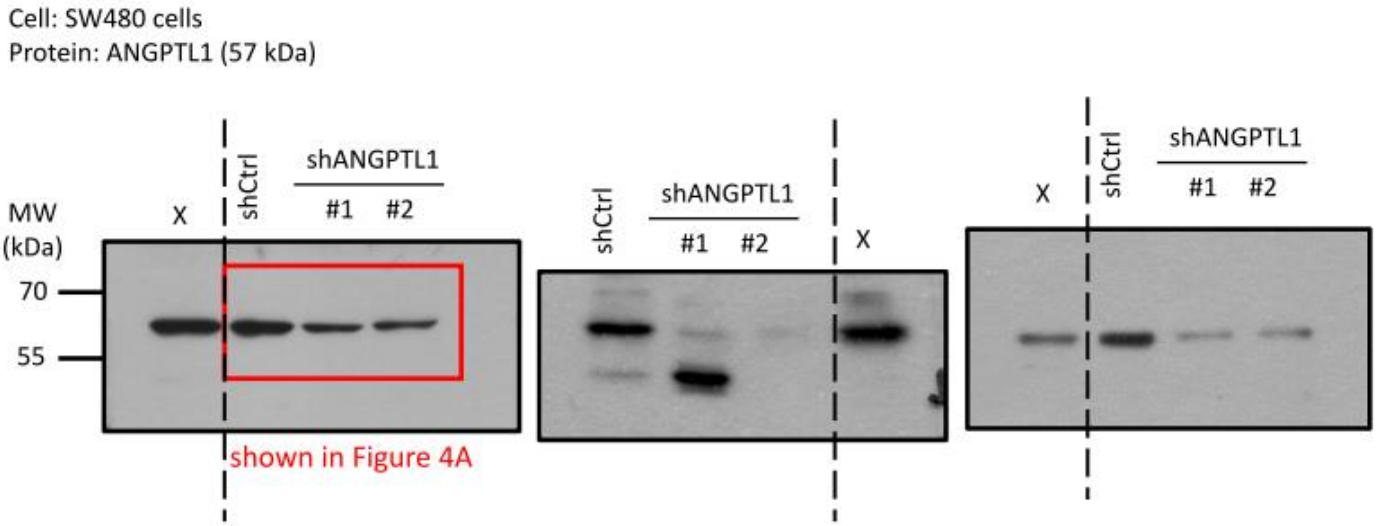

19. Figure 4A-right

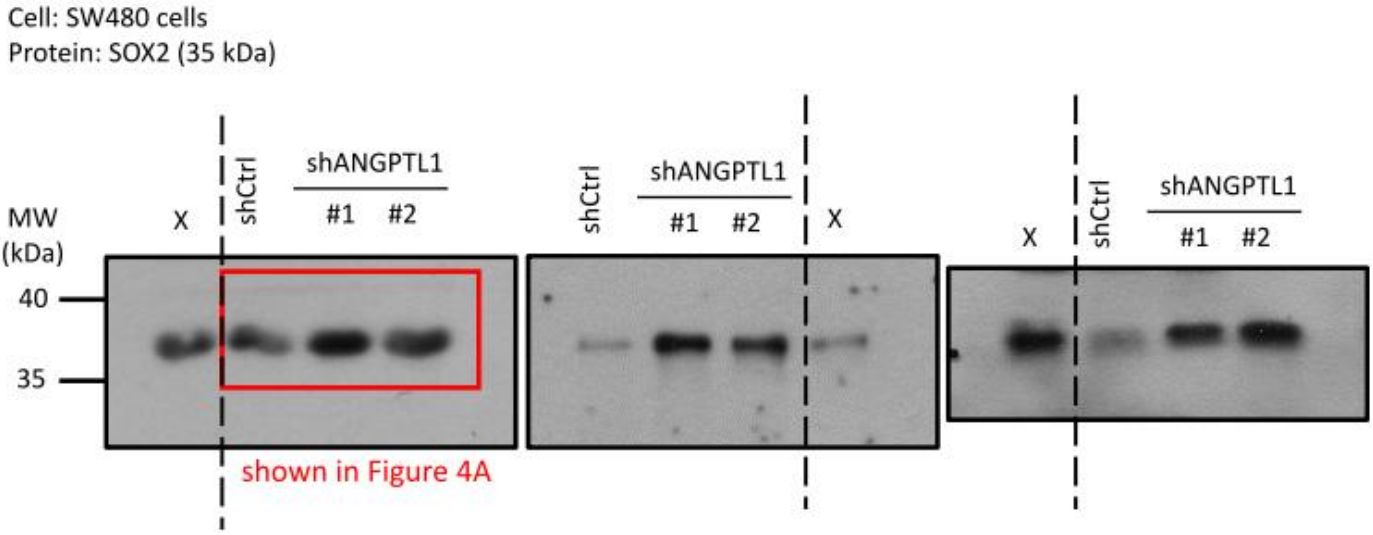

20. Figure 4A-right

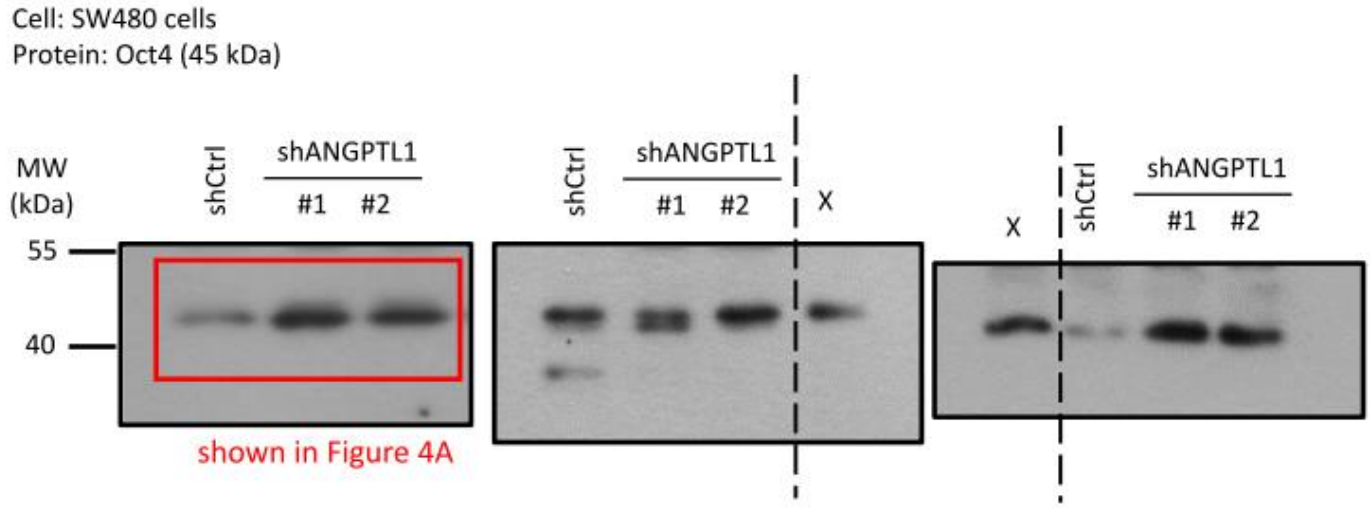

21. Figure 4A-right

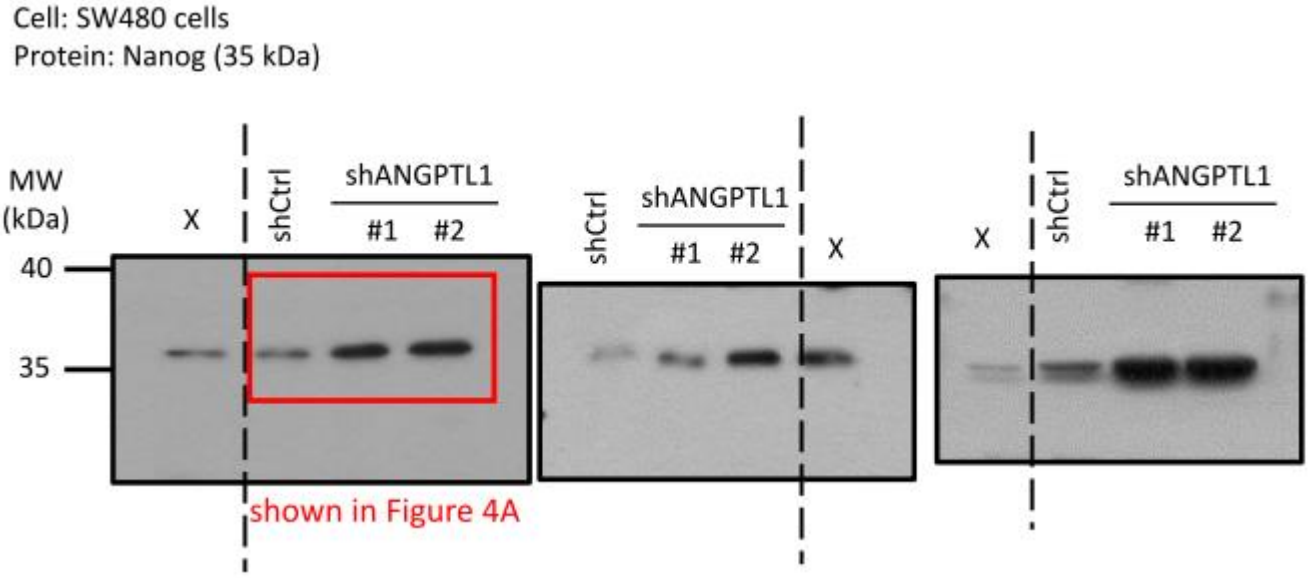

22. Figure 4A-right

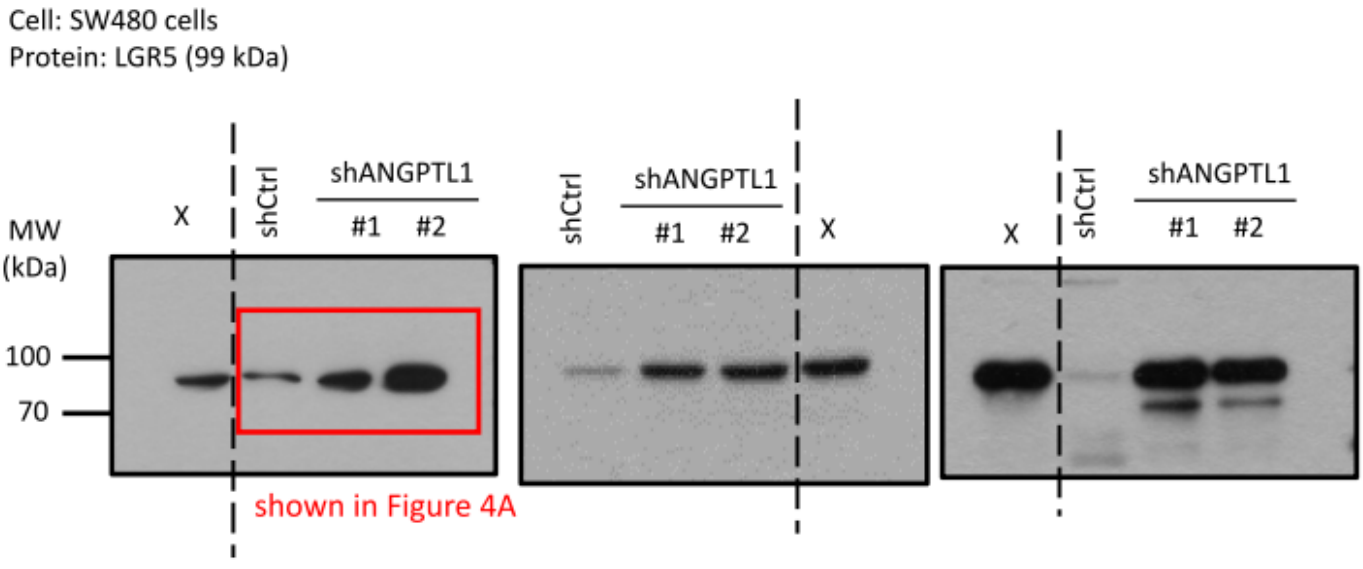

23. Figure 4A-right

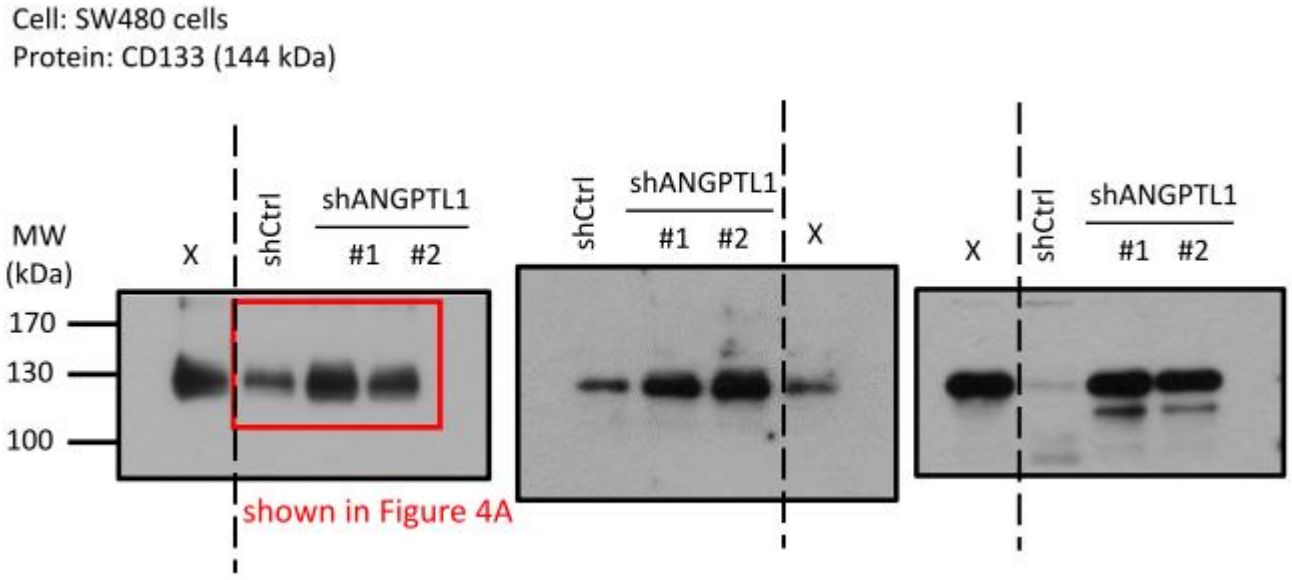

24. Figure 4A-right

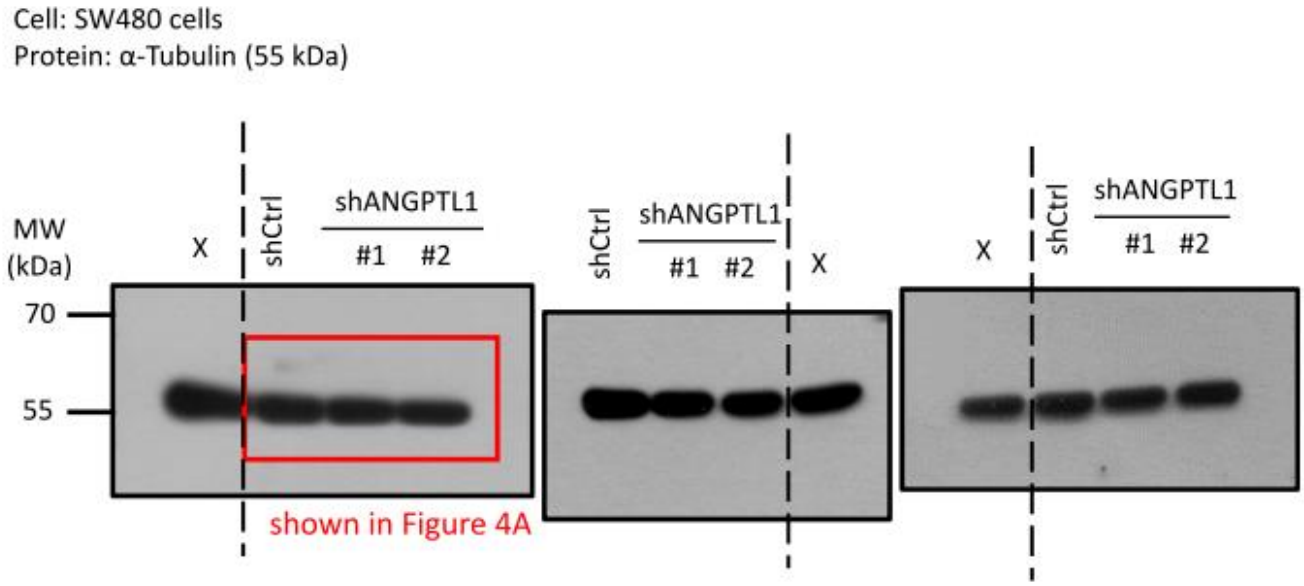

25. Figure 4C

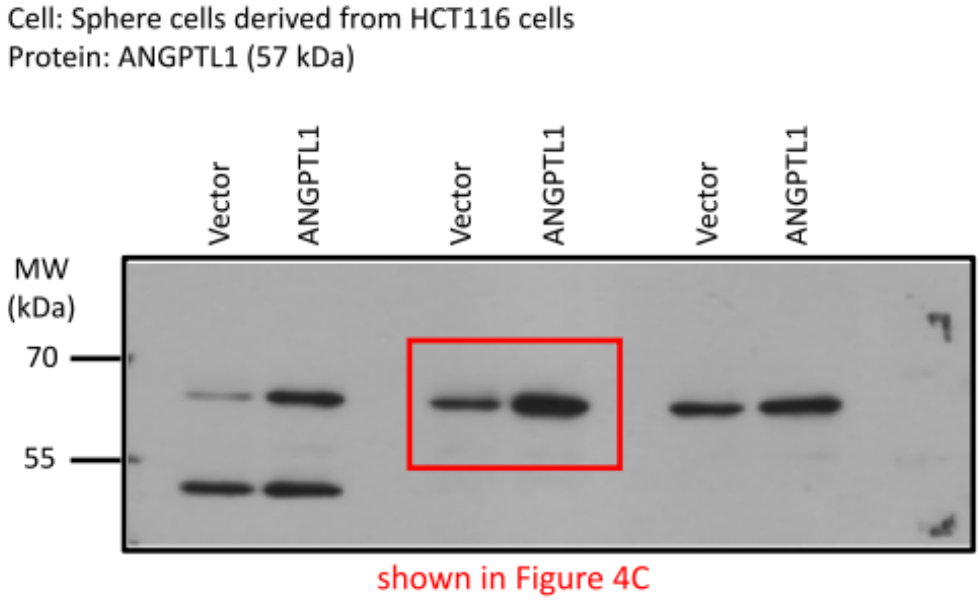

26. Figure 4C

Cell: Sphere cells derived from HCT116 cells
Protein: SOX2 (35 kDa)

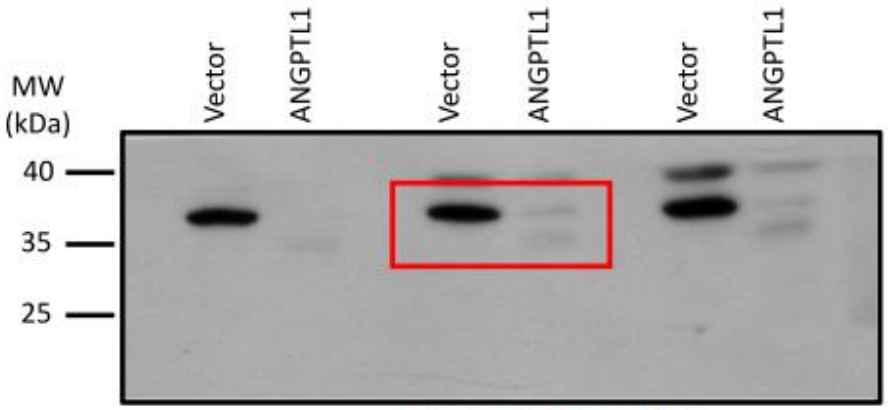

shown in Figure 4C

27. Figure 4C

Cell: Sphere cells derived from HCT116 cells
Protein: Oct4 (45 kDa)

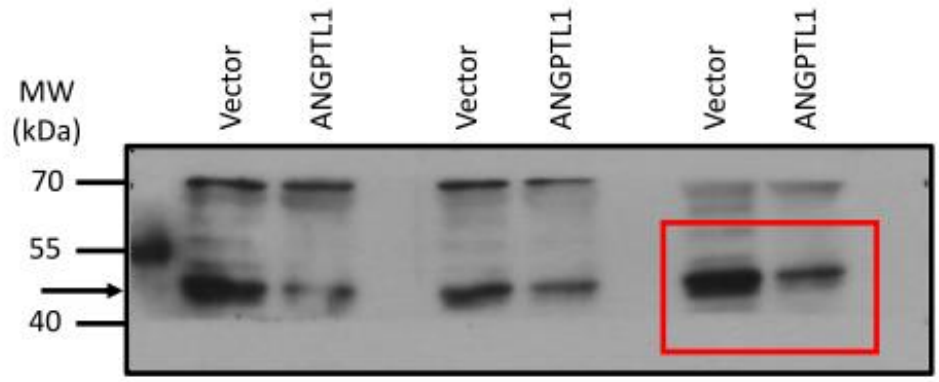

shown in Figure 4C

28. Figure 4C

Cell: Sphere cells derived from HCT116 cells
Protein: Nanog (35 kDa)

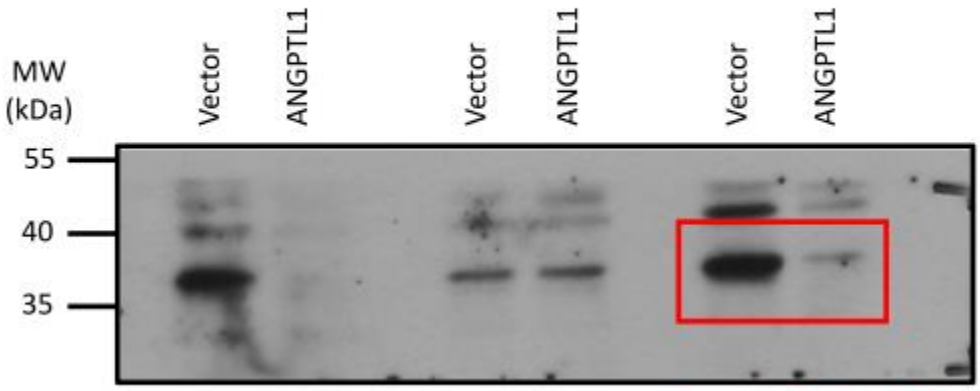

shown in Figure 4C

29. Figure 4C

Cell: Sphere cells derived from HCT116 cells
Protein: LGR5 (99 kDa)

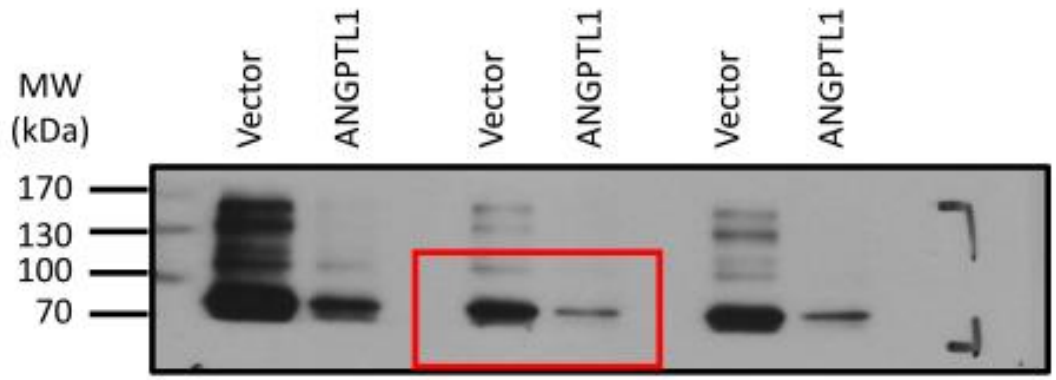

shown in Figure 4C

30. Figure 4C

Cell: Sphere cells derived from HCT116 cells
Protein: CD133 (144 kDa)

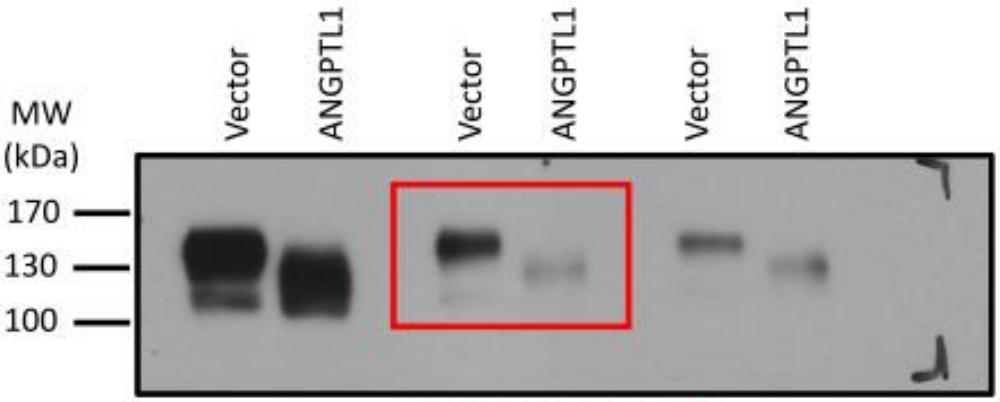

shown in Figure 4C

31. Figure 4C

Cell: Sphere cells derived from HCT116 cells
Protein: α-Tubulin (55 kDa)

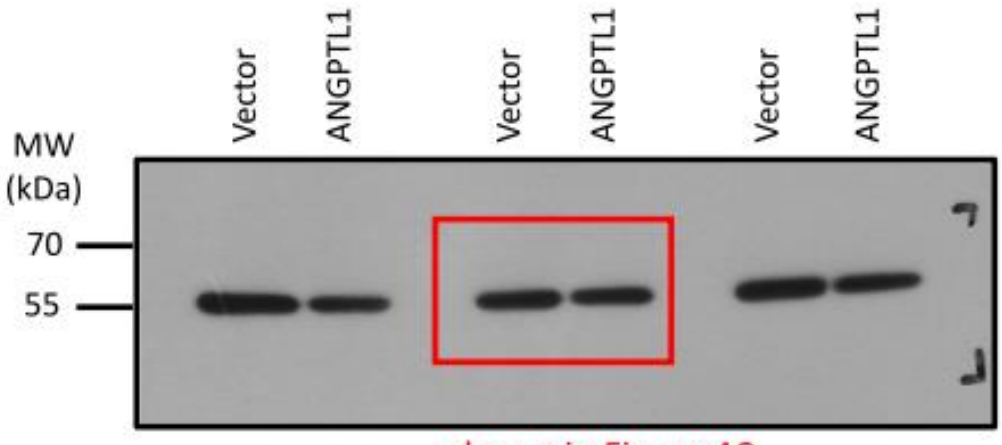

shown in Figure 4C

32. Figure 4E

Cell: Sphere cells derived from SW480 cells
Protein: ANGPTL1 (57 kDa)

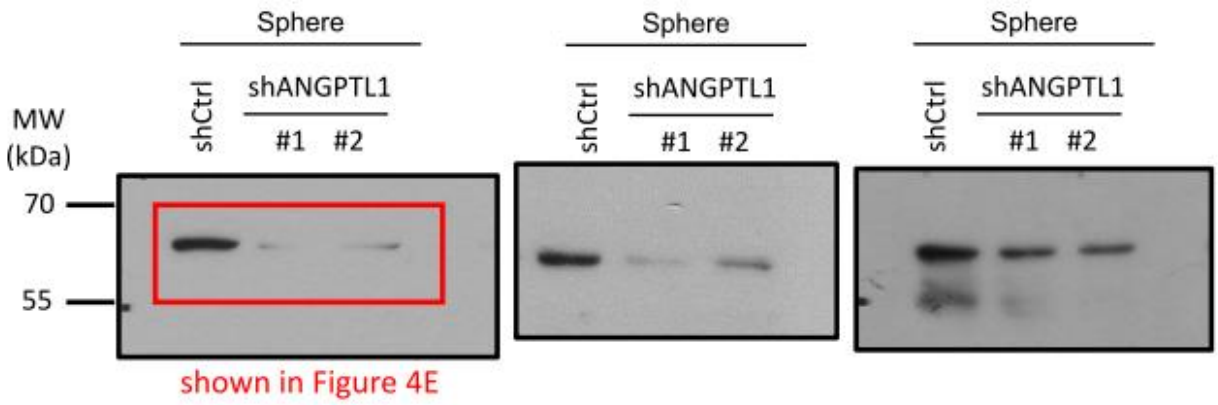

shown in Figure 4E

33. Figure 4E

Cell: Sphere cells derived from SW480 cells
Protein: SOX2 (35 kDa)

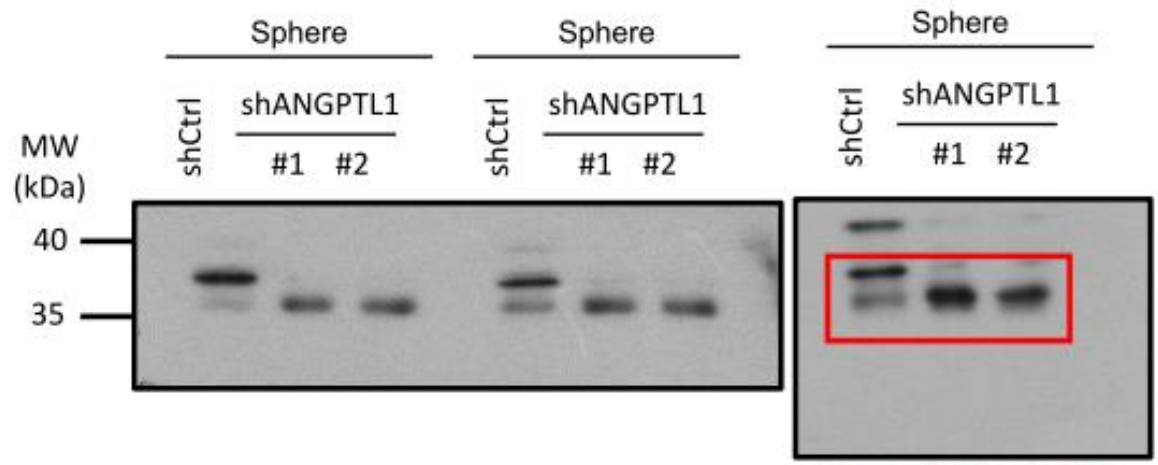

shown in Figure 4E

34. Figure 4E

Cell: Sphere cells derived from SW480 cells
Protein: Oct4 (45 kDa)

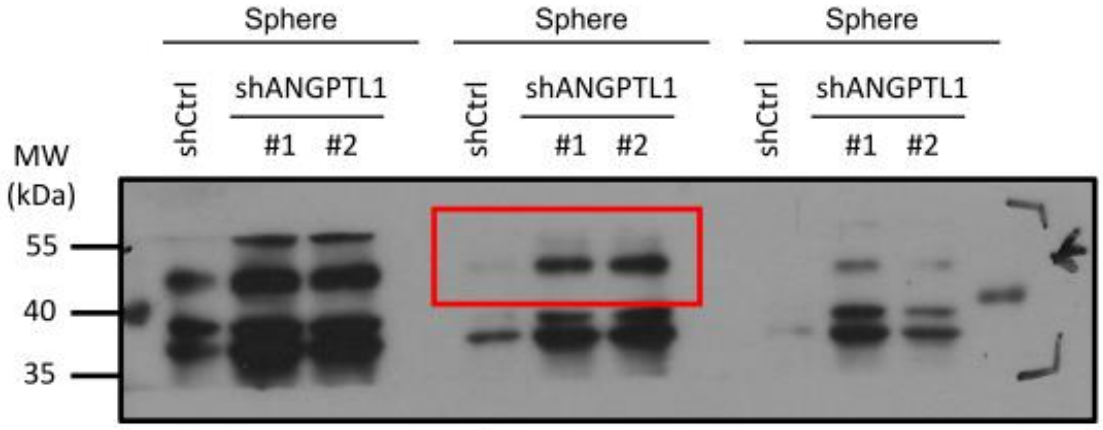

shown in Figure 4E

35. Figure 4E

Cell: Sphere cells derived from SW480 cells
Protein: Nanog (35 kDa)

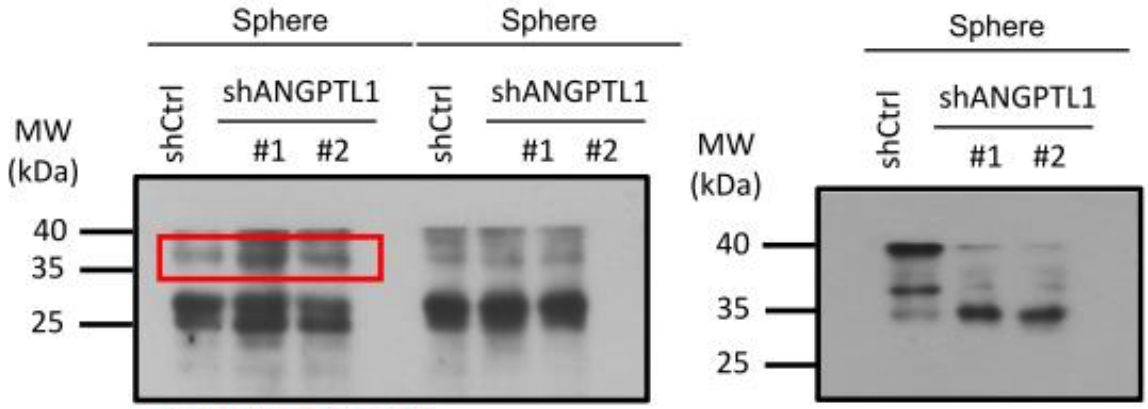

shown in Figure 4E

36. Figure 4E

Cell: Sphere cells derived from SW480 cells
Protein: LGR5 (99 kDa)

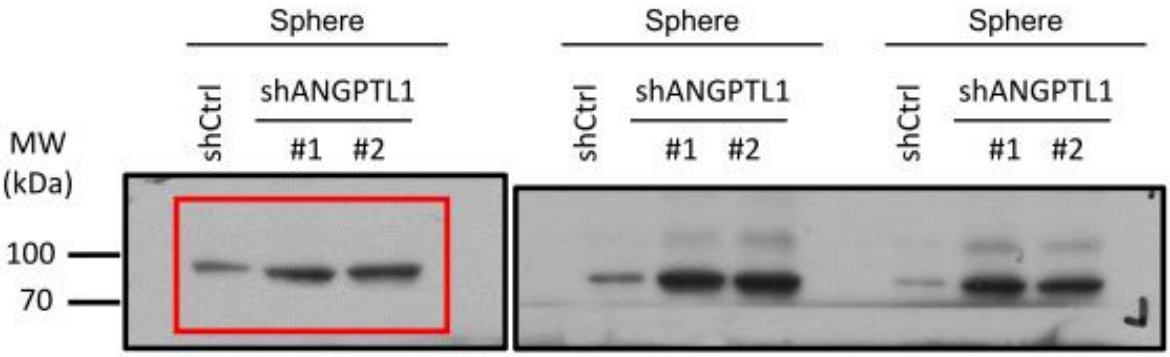

shown in Figure 4E

37. Figure 4E

Cell: Sphere cells derived from SW480 cells
Protein: CD133 (144 kDa)

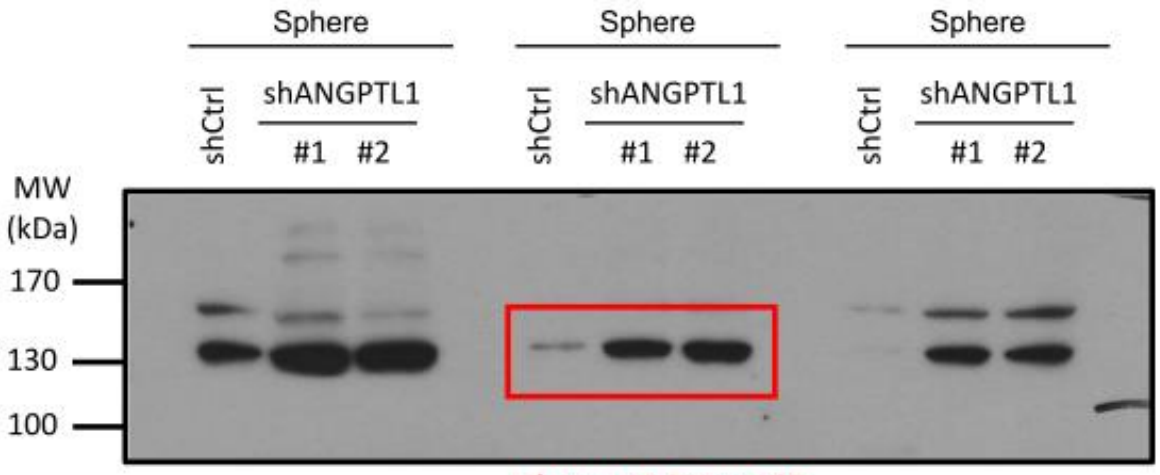

shown in Figure 4E

38. Figure 4E

Cell: Sphere cells derived from SW480 cells
Protein: α-Tubulin (55 kDa)

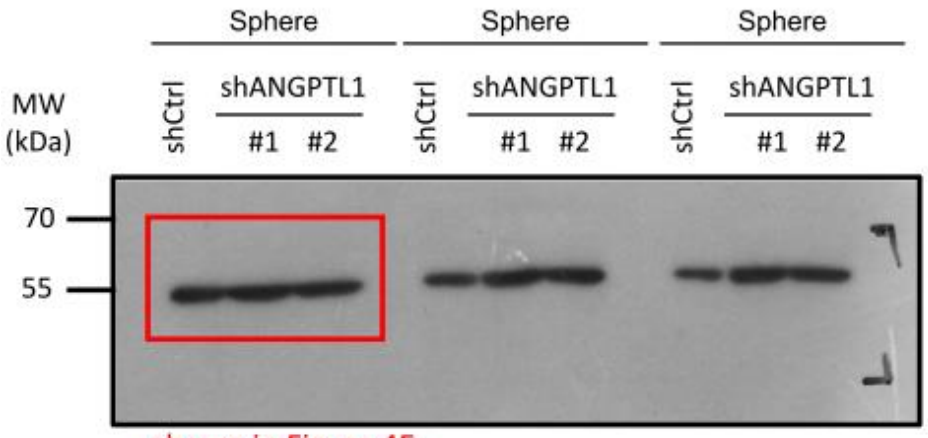

shown in Figure 4E

39. Figure 5A

Cell: HCT116 cells
Protein: FOXO1 (70 kDa)

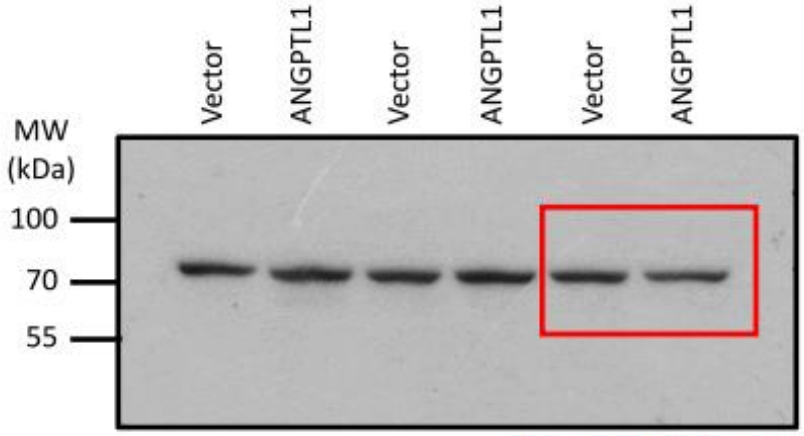

shown in Figure 5A

40. Figure 5A

Cell: HCT116 cells
Protein: FOXO3a (90 kDa)

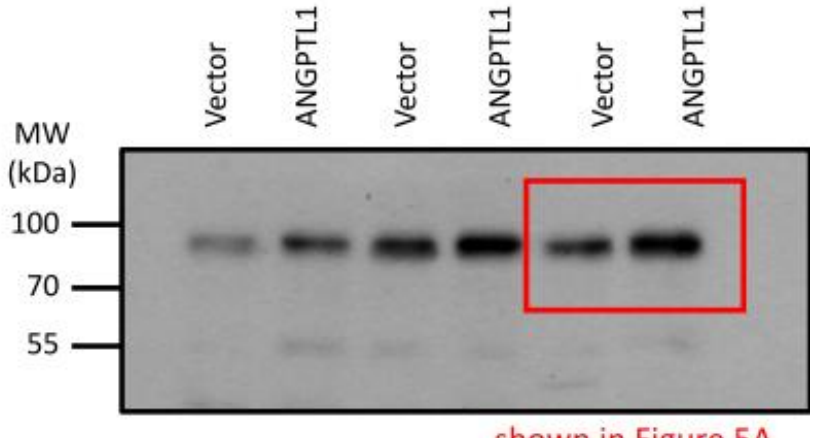

shown in Figure 5A

41. Figure 5A

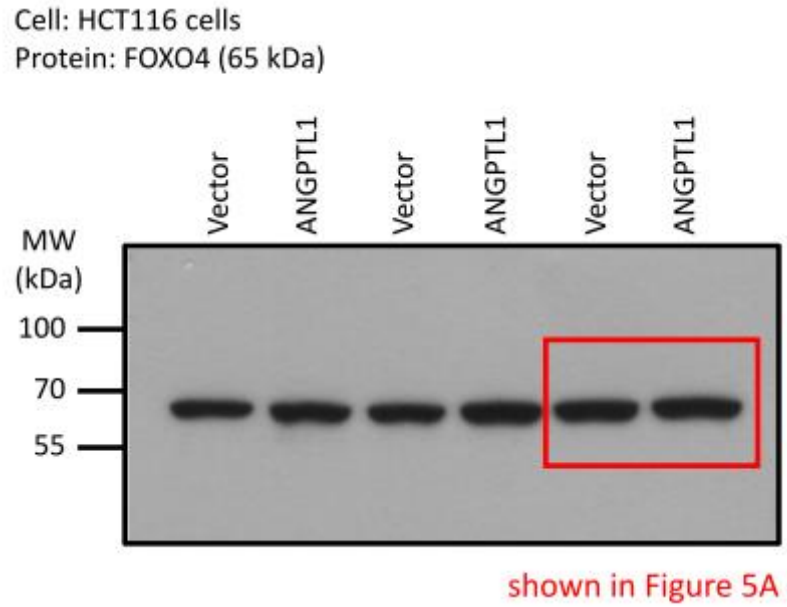

42. Figure 5A

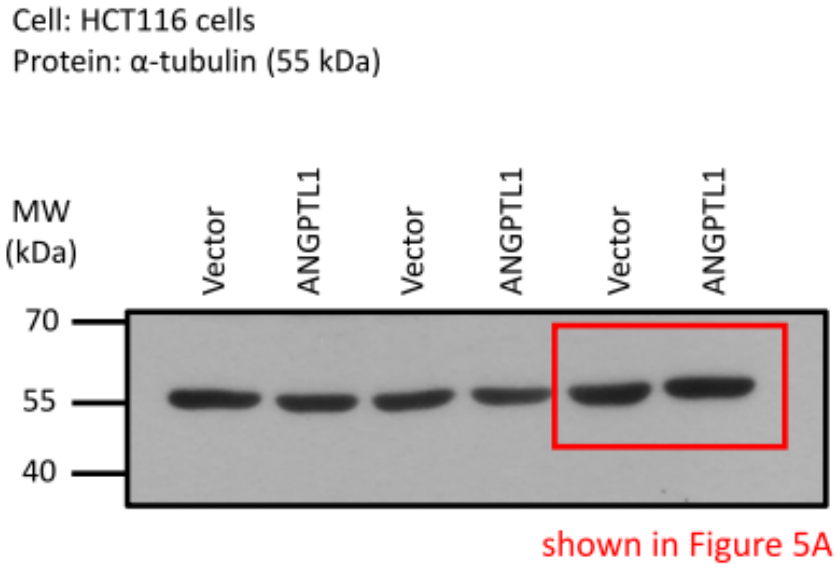

43. Figure 5C

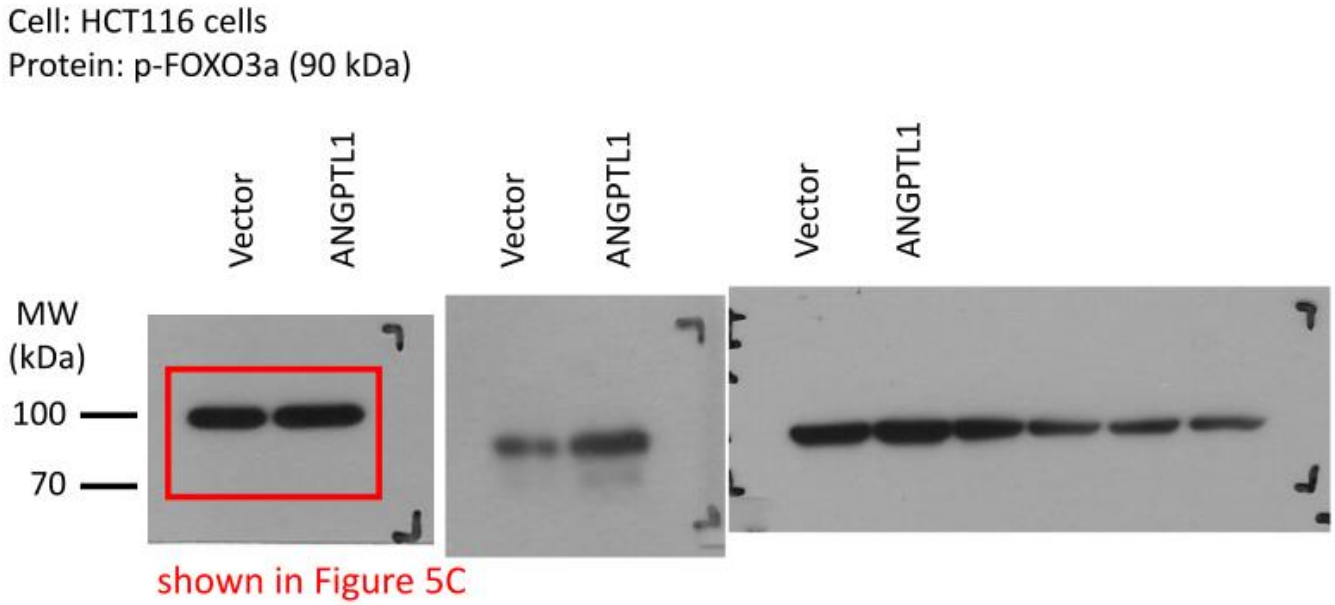

44. Figure 5C

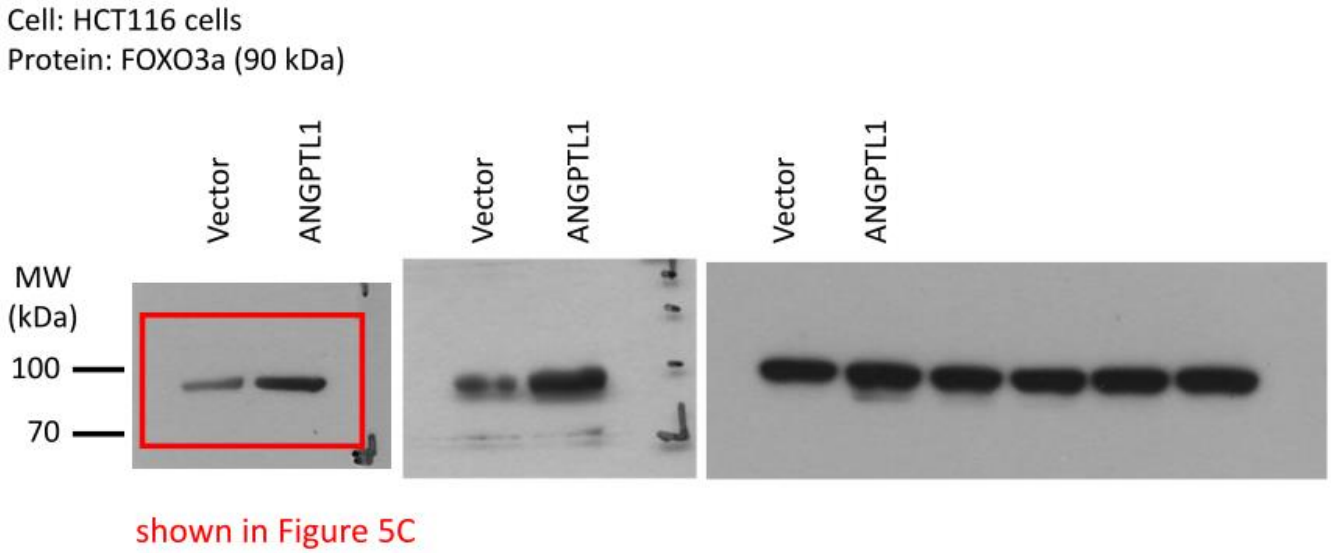

45. Figure 5C

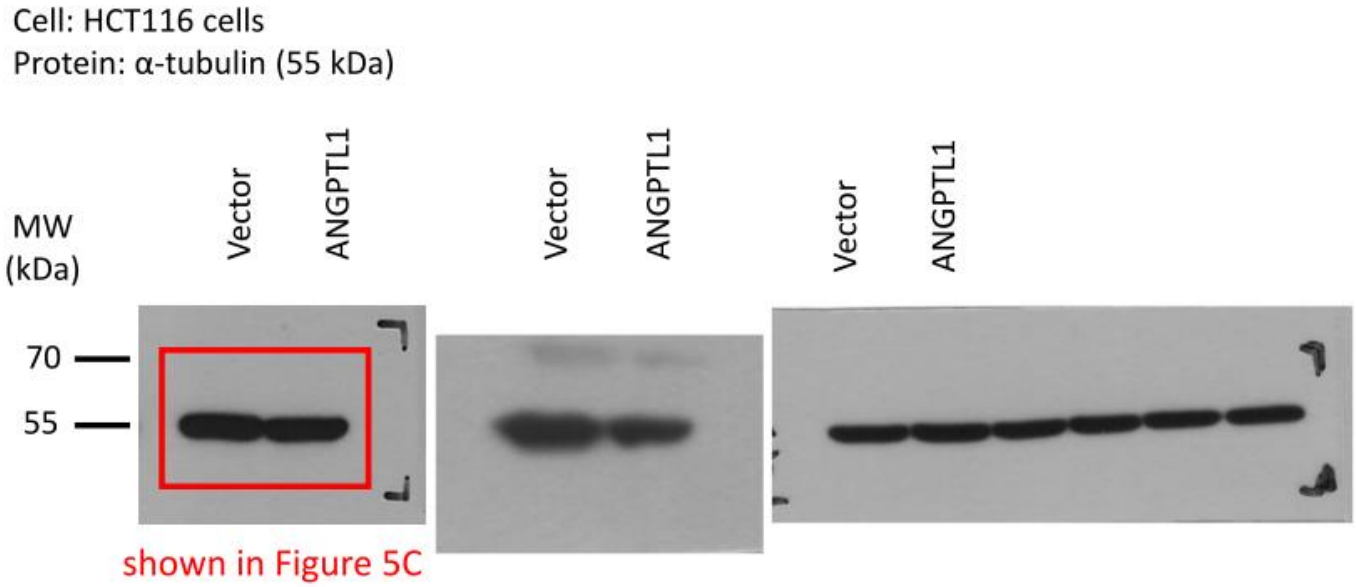

46. Figure 5D

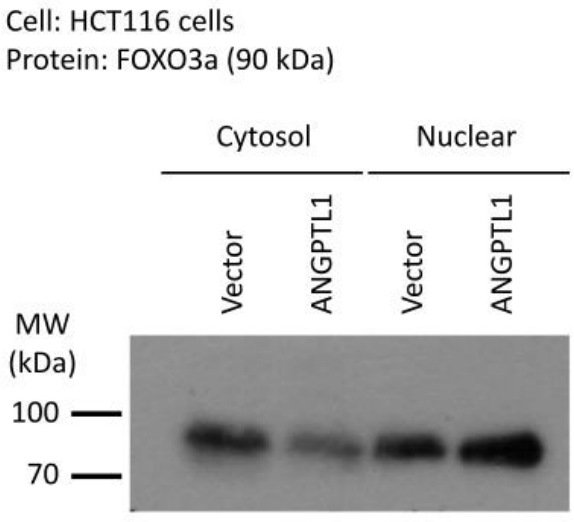

47. Figure 5D

Cell: HCT116 cells
Protein: Lamin A/C (74/63 kDa)

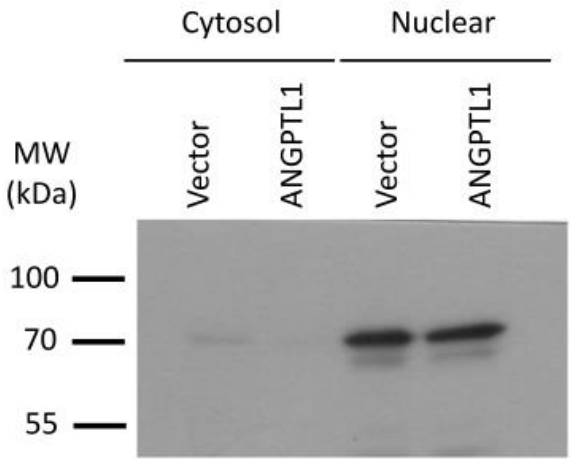

48. Figure 5D

Cell: HCT116 cells
Protein: α-tubulin (55 kDa)

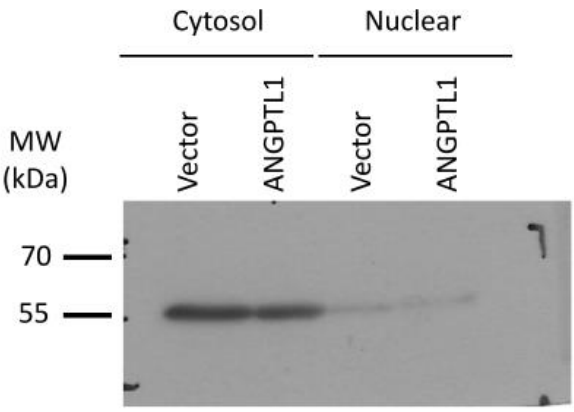

49. Figure 5E

Cell: HCT116 cells
Protein: ANGPTL1 (57 kDa)

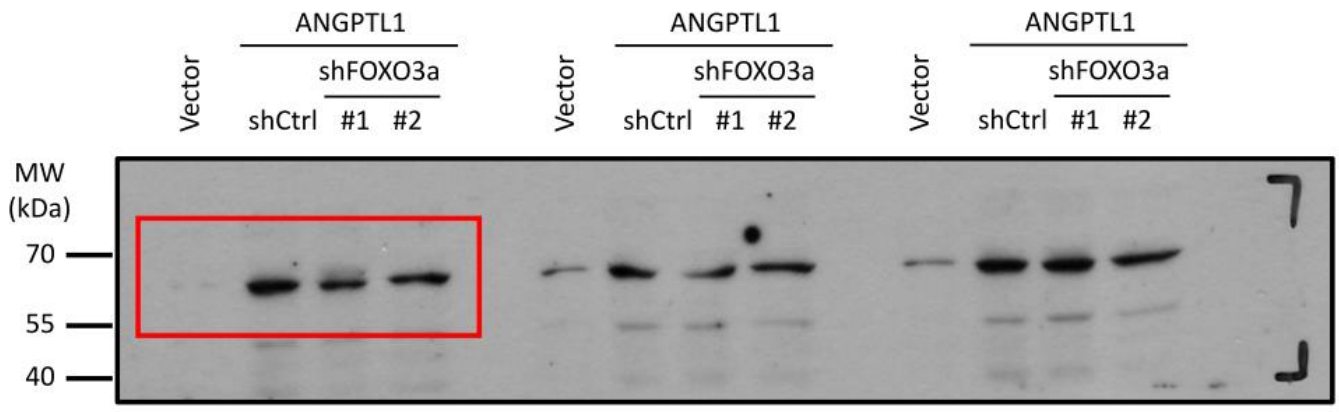

shown in Figure 5E

50. Figure 5E

Cell: HCT116 cells
Protein: FOXO3a (90 kDa)

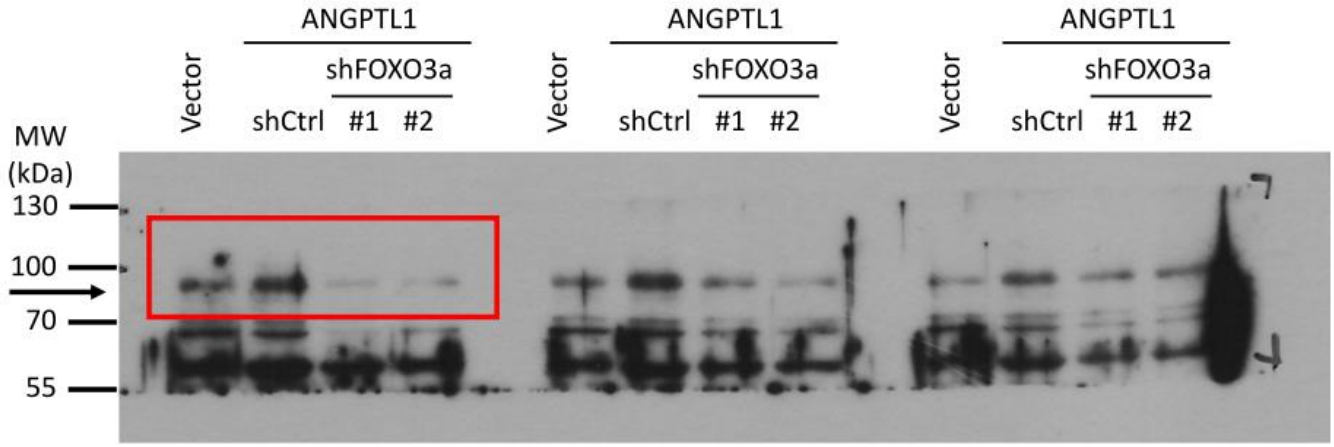

shown in Figure 5E

51. Figure 5E

Cell: HCT116 cells
Protein: α-tubulin (55 kDa)

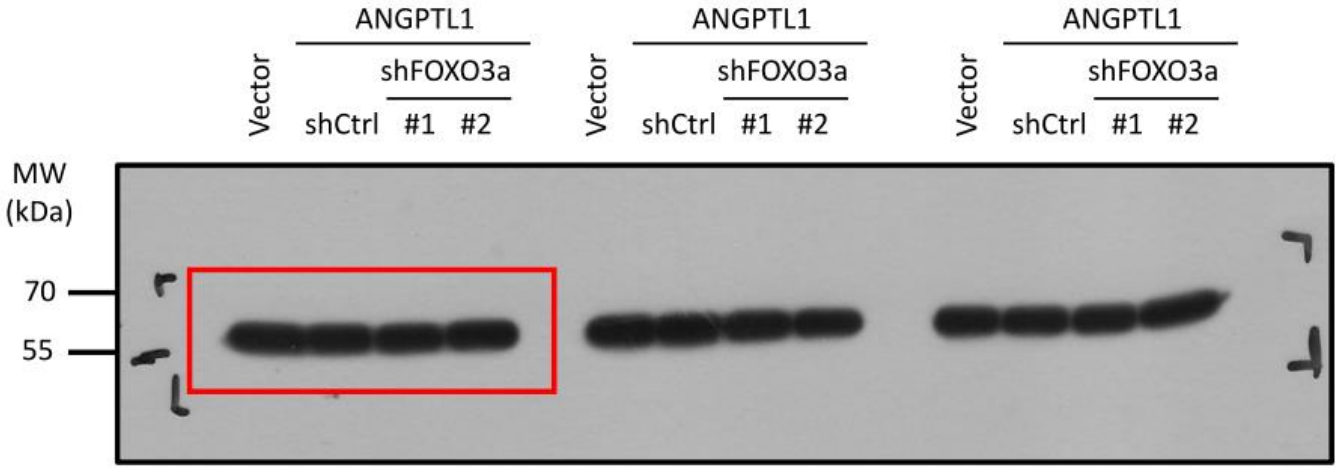

shown in Figure 5E

52. Figure 6A

Cell: HCT116 cells
Protein: ANGPTL1 (57 kDa)

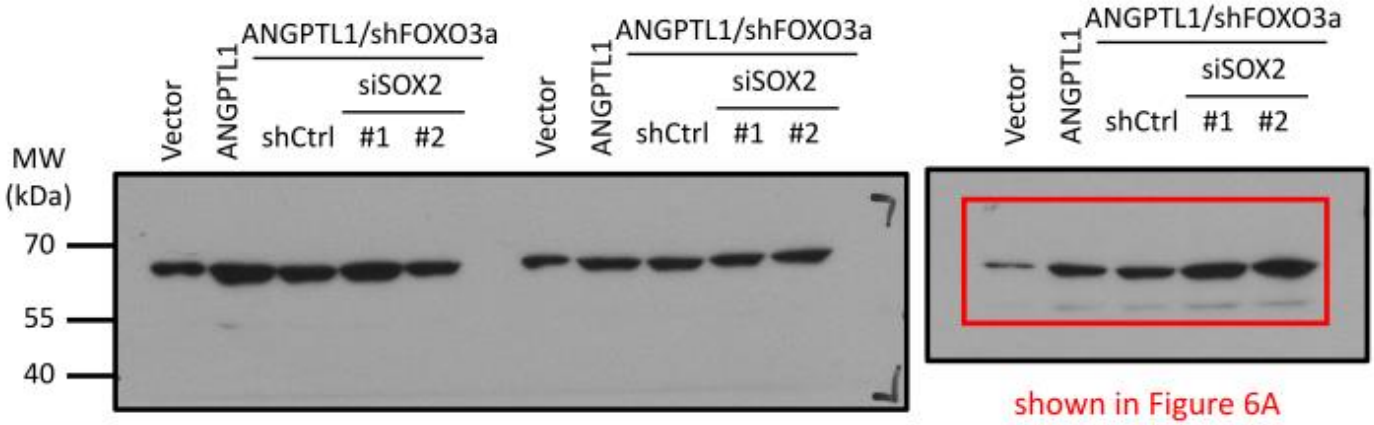

shown in Figure 6A

53. Figure 6A

Cell: HCT116 cells
Protein: FOXO3a (90 kDa)

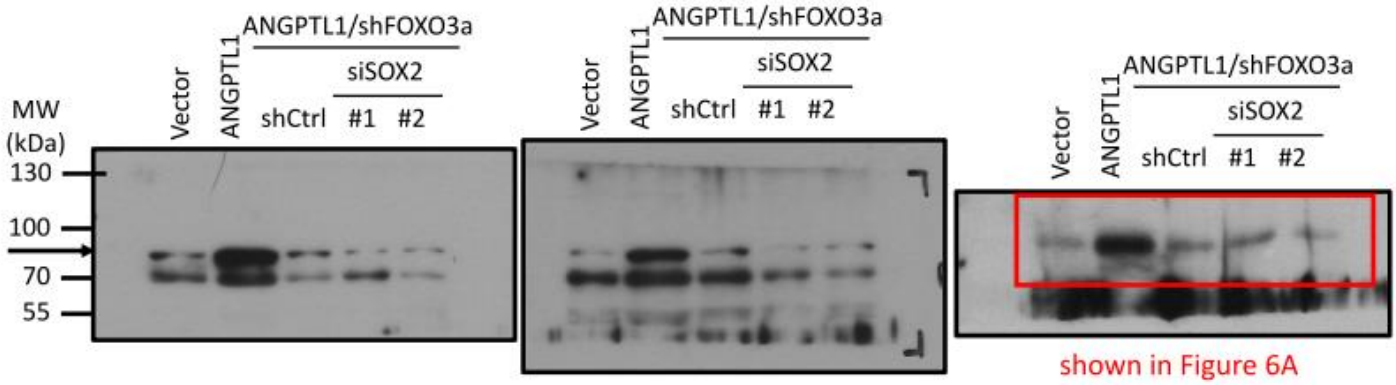

54. Figure 6A

Cell: HCT116 cells
Protein: SOX2 (35 kDa)

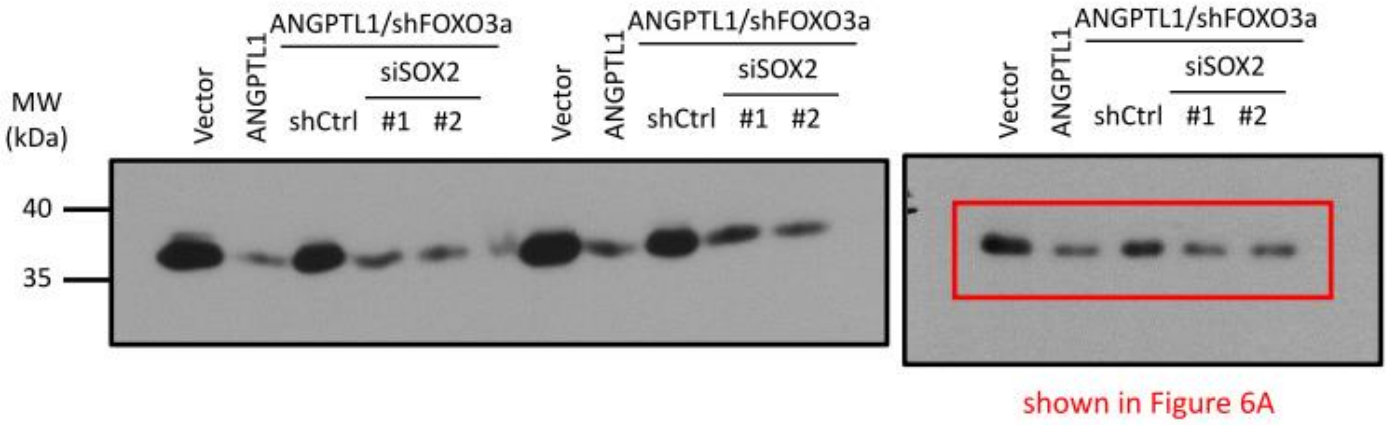

55. Figure 6A

Cell: HCT116 cells
Protein: α-tubulin (55 kDa)